

Session 2: Effects of joint action on frames 1

Objekttyp: **Group**

Zeitschrift: **IABSE reports = Rapports AIPC = IVBH Berichte**

Band (Jahr): **75 (1996)**

PDF erstellt am: **07.07.2024**

Nutzungsbedingungen

Die ETH-Bibliothek ist Anbieterin der digitalisierten Zeitschriften. Sie besitzt keine Urheberrechte an den Inhalten der Zeitschriften. Die Rechte liegen in der Regel bei den Herausgebern.

Die auf der Plattform e-periodica veröffentlichten Dokumente stehen für nicht-kommerzielle Zwecke in Lehre und Forschung sowie für die private Nutzung frei zur Verfügung. Einzelne Dateien oder Ausdrucke aus diesem Angebot können zusammen mit diesen Nutzungsbedingungen und den korrekten Herkunftsbezeichnungen weitergegeben werden.

Das Veröffentlichen von Bildern in Print- und Online-Publikationen ist nur mit vorheriger Genehmigung der Rechteinhaber erlaubt. Die systematische Speicherung von Teilen des elektronischen Angebots auf anderen Servern bedarf ebenfalls des schriftlichen Einverständnisses der Rechteinhaber.

Haftungsausschluss

Alle Angaben erfolgen ohne Gewähr für Vollständigkeit oder Richtigkeit. Es wird keine Haftung übernommen für Schäden durch die Verwendung von Informationen aus diesem Online-Angebot oder durch das Fehlen von Informationen. Dies gilt auch für Inhalte Dritter, die über dieses Angebot zugänglich sind.



SESSION 2
EFFECTS OF JOINT ACTION ON FRAMES 1

Leere Seite
Blank page
Page vide



Investigation on the validity of connection classification system

Norimitsu KISHI
Associate Professor
Muroran Inst. of Technology
Muroran, Japan 050

Rafiq HASAN
Post Doctoral Fellow
Muroran Inst. of Technology
Muroran, Japan 050

Yoshiaki GOTO
Professor
Nagoya Inst. of Technology
Nagoya, Japan 466

Masato KOMURO
Research Associate
Muroran Inst. of Technology
Muroran, Japan 050

Summary

The rationale used to devise connection classification systems (EC3, 1992 and BJORHOVDE et al., 1990) is that: the connection stiffness should be compared with beam stiffness. It is shown by performing frame analysis that this rationale is plausible but does not produce satisfactory results. Therefore, this study stems the rationale and shows the necessity of having a classification system which reasonably reflects the proper contributions of the connection components on connection behavior.

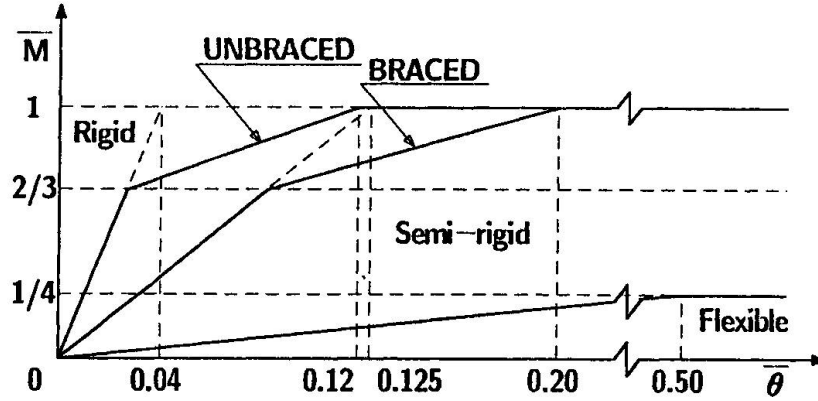
1. Introduction

In steel construction, beam-to-column connections are commonly classified into three categories: (i) rigid connection, (ii) semi-rigid connection, and (iii) flexible connection. In North American codes, this classification is described in general terms without explicitly defining the connections in terms of connection strength or stiffness. On the other hand, as a unified effort in Europe, a systematic connection classification scheme was introduced in their EC3 (1992) code. Among other contemporary efforts on connection classification, BJORHOVDE et al.'s (1990) classification system received keen attention. In both classification systems, moment axis is non-dimensionalized with reference to the plastic moment of the connected beam. The rotation axis is non-dimensionalized with reference to the stiffness either of the full length or of a reference length of the beam. These appear to be the contrary to the common experimental evidences that the moment-rotation behaviors of steel connections are mainly dependent on the characteristics of the connection elements (such as: geometric and material properties of angle, plate, fastener, column flange etc.) rather than the properties of connecting beam.

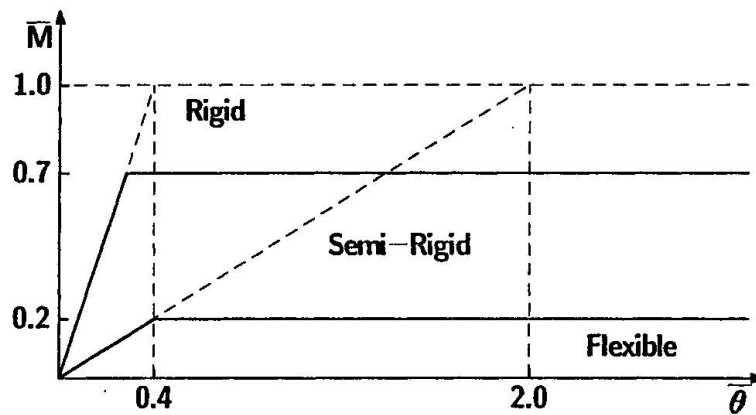
In this study, these skepticisms regarding the validity of the classification systems (EC3 and BJORHOVDE et al.) have been examined by conducting frame analysis. To this end, a second-order elastic analysis program which considers non-linear connection stiffness is used. In the frame analysis, a good number of experimental



moment-rotation curves as well as those obtained from the classification schemes are used. The frame responses obtained by applying the experimental moment-rotation curves are compared with the results correspond to the classification schemes. From the comparison, the validity of the classification schemes, with reference to initial connection stiffness, has been examined.



(a) EC3 classification



(b) Bjorhovde et al.'s classification

Fig. 1. Connection classification systems

2. Connection classification systems

The non-dimensional moment-rotation classification system as per the EC3 (1992) and Bjorhovde et al. (1990) are illustrated in Fig. 1. Main features of the classification systems can be listed as:

- 1) The moment axis is non-dimensionalized with reference to plastic moment of the connected beam M_p , i.e.,

$$\bar{M} = M/M_p \quad (1)$$

- 2) The rotation axis is non-dimensionalized with reference to reference plastic rotation θ_p , i.e.,

$$\bar{\theta} = \theta/\theta_p \quad (2)$$

where plastic rotation is defined as the beam stiffness either of full length (EC3) or of a reference length (Bjorhovde et al.), i.e.,

$$\text{EC3:} \quad \theta_p = M_p/(EI/L) \quad (3)$$

$$\text{Bjorhovde et al.:} \quad \theta_p = M_p/(EI/5d) \quad (4)$$

where L and d are the beam length and depth, respectively.

- (3) The EC3 classification system recognizes different semi-rigid action depending upon the type of the structure, i.e., braced or unbraced frame and provides different boundary lines between rigid and semi-rigid connections (Fig. 1a). On the other hand, same boundary line is provided between semi-rigid and flexible connections for both types of frames.

2.1 Initial connection stiffness as per classification systems

The boundary values of initial connection stiffnesses of the rigid, semi-rigid and flexible connections can be calculated from the primary slopes of the boundary lines among the three connection categories as shown in Fig. 1 are listed in Table 1. The major drawbacks of the classification systems are well manifested in this table: the initial connection stiffness, instead of depending on the properties of connection elements, completely depends on the physical and material properties of the connected beam. For the same connection configuration, as per the EC3 classification system, a change in beam length causes a change in initial connection stiffness. Similarly, Bjorhovde et al.'s classification suggests that a change in beam depth results in a variation in the value of initial connection stiffness without referring to connection details or properties of connection elements. These, obviously, do not pertain to the reality. Therefore, the validity of the classification systems is not beyond question and requires examination.

Table 1. Boundary values of initial connection stiffness of different connections

Initial Connection Stiffness (R_{ki})	EC3		Bjorhovde et al.
	unbraced	braced	
minimum R_{ki} of rigid connection or maximum R_{ki} of semi-rigid connection	$R_{ki} = \frac{25EI}{L}$	$R_{ki} = \frac{8EI}{L}$	$R_{ki} = \frac{EI}{2d}$
minimum R_{ki} of semi-rigid connection or maximum R_{ki} of flexible connection	$R_{ki} = \frac{EI}{2L}$		$R_{ki} = \frac{EI}{10d}$

3. Methodology

As evident from Table 1, two primary slopes can be identified as: (i) minimum initial connection stiffness of a rigid connection and (ii) maximum initial connection stiffness of a flexible connection. The validity of the two theoretical boundary values is examined by comparing with the experimental boundary values obtained from frame analysis.

3.1 Minimum initial connection stiffness of a rigid connection

Extended end-plate connection, a typical of which is shown in Fig. 2(a), consists of a end-plate profile welded to the beam end, bolted to the column flange and extended beyond the beam flange. This type of connection is commonly used to sustain high moment and is generally regarded as rigid connection. Therefore, a total of 112 experimental moment-rotation curves of this connection stored in the updated data base (Hasan et al., 1995) are utilized to determine the experimental minimum initial connection stiffness of a rigid connection. To this end, a second-order elastic analysis



program considering non-linear connection stiffness (Goto and Chen, 1987) is used to calculate the frame responses (beam end moments and frame drift). Calculated values for real connections are normalized by the corresponding values for rigid connections i.e.,

$$\text{normalized beam end moment, } m^* = \frac{\text{moment for extended end-plate connection}}{\text{moment for fully rigid connection}}$$

$$\text{normalized frame drift, } d^* = \frac{\text{drift for extended end-plate connection}}{\text{drift for fully rigid connection}}$$

Normalized beam end moment m^* and normalized frame drift d^* are then plotted against initial connection stiffness R_{kj} . Relative locations of the data correspond to the EC3 and Bjorhovde et al. classification systems are also shown in these figures by black star and triangular marks, respectively, as shown in section 4. Frame analyses are executed by using portal; two-bay two-story and four-bay two-story frames as shown in Fig. 4. In these frames, W21x44 for floor beam and W14x22 for roof beam are used. The moment-rotation relations for these beam sections correspond to each classification systems are shown in Fig. 3(a).

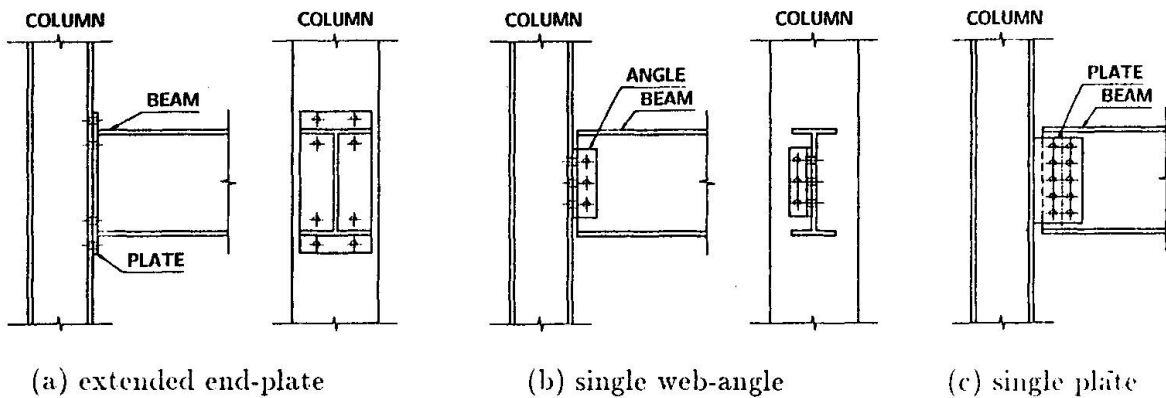


Fig. 2. Practical connections used in frame analysis

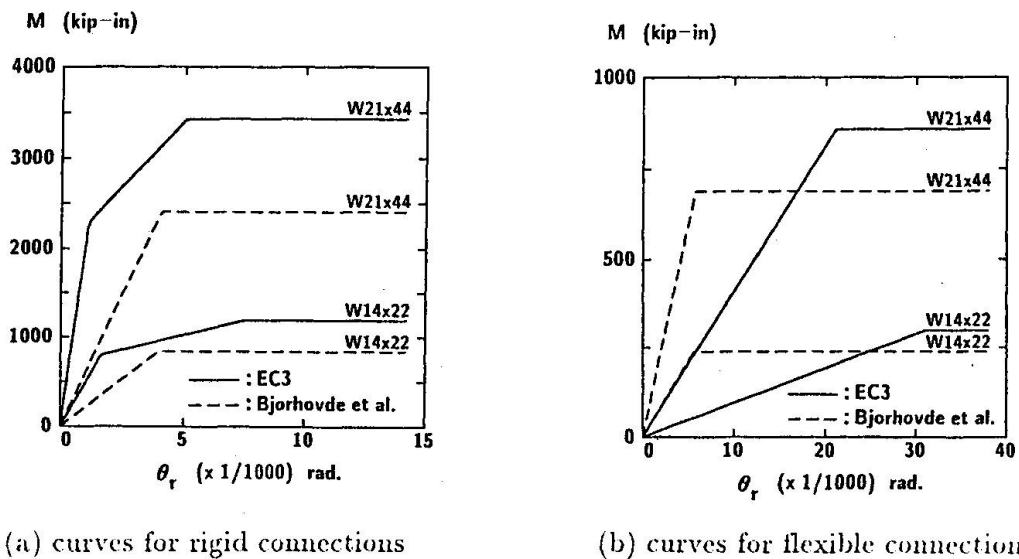


Fig. 3. Moment-rotation curves as per classification system

3.2 Maximum initial connection stiffness of a flexible connection

To examine the validity of classification systems with reference to stiffness of flexible connection, same procedure is followed as described in the sub-section 3.1. The practical connections used for this purpose are: (i) single web-angle connection and (ii) single plate connection, because they are generally regarded as flexible connections. These connections use only one angle/plate in the web of the beam as shown in Figs. 2(b) and (c). The frame responses (mid-span moment and frame drift) obtained from frame analysis are normalized as follows:

$$\text{normalized mid-span moment, } m^* = \frac{\text{moment for single web-angle/plate connection}}{\text{moment for flexible connection}}$$

$$\text{normalized frame drift, } d^* = \frac{\text{drift for single web-angle/plate connection}}{\text{drift for flexible connection}}$$

For moment analysis, mid-span moments are considered because the end moments of a beam element are almost zero when it is connected to the column with flexible connections. A total of 54 experimental moment-rotation curves stored in the updated data base (Hasan et al., 1995) are utilized to calculate frame responses correspond to real connections. The same frames (Fig. 4) used for rigid connection analysis are used here. The moment-rotation curves as per classification systems for floor beam (W21×44) and roof beam (W14×22) are shown in Fig. 3(b), respectively.

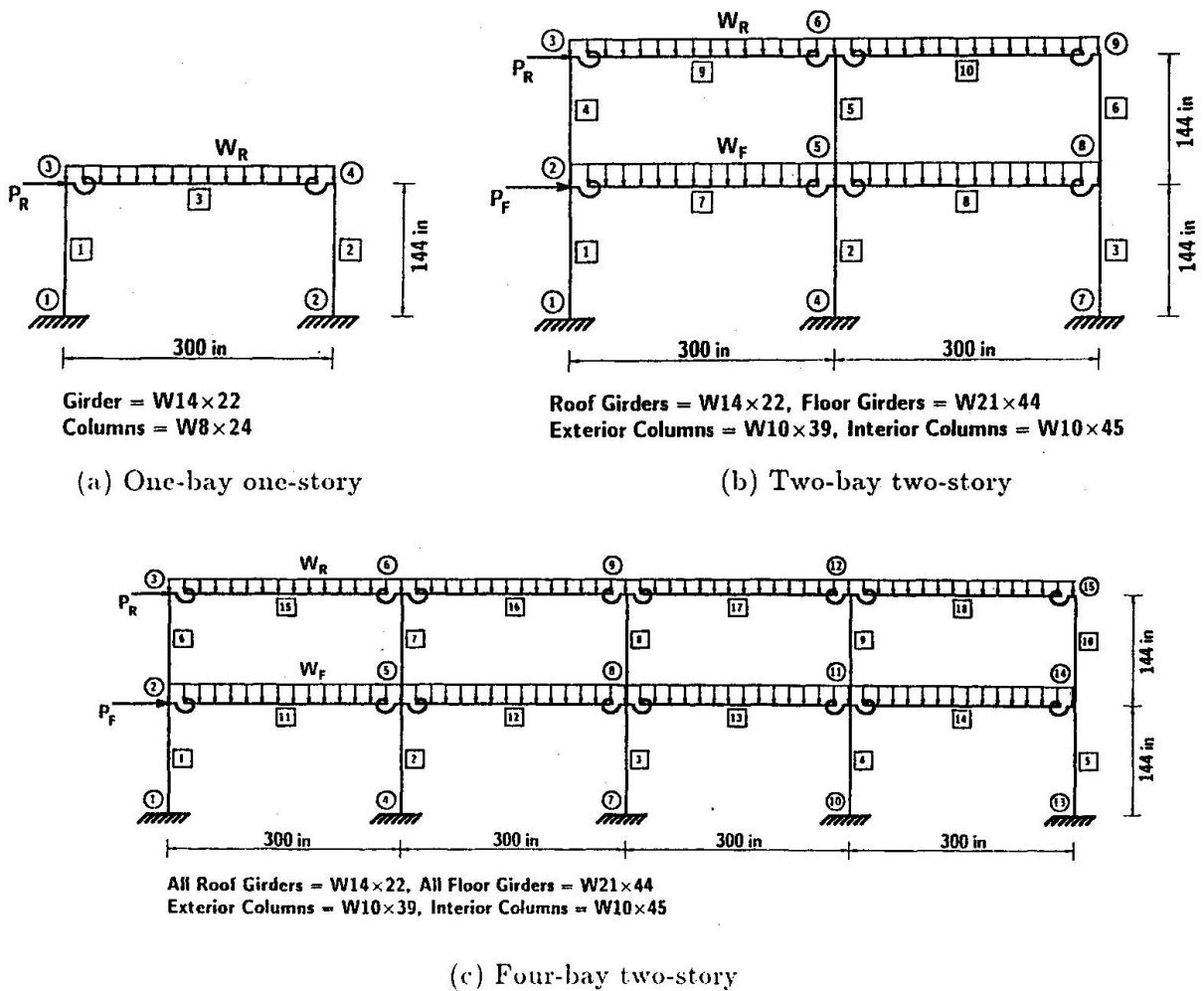


Fig. 4. Frames used in analysis



4. Frame analysis

Three frames: one-bay one-story, two-bay two-story and four-bay two-story, as shown in Fig. 4 are analyzed. Beam and column sections, floor heights and beam spans used are shown in their corresponding figures. Element nos. are shown in boxes while node nos. are shown in circles. The frames are loaded with 68 and 48 psf load as floor dead (D) and live (L) load, respectively. The intensity of roof dead (D) and live (L) load, and wind (W) load are of equal magnitude: 20 psf. Frame drift and end/mid-span beam moments are obtained for service load combination (D+L+W) and factored load combination (1.2D+0.5L+1.3W), respectively, as per AISC-LRFD specification (1994). The frame spacing is taken as 300 inch.

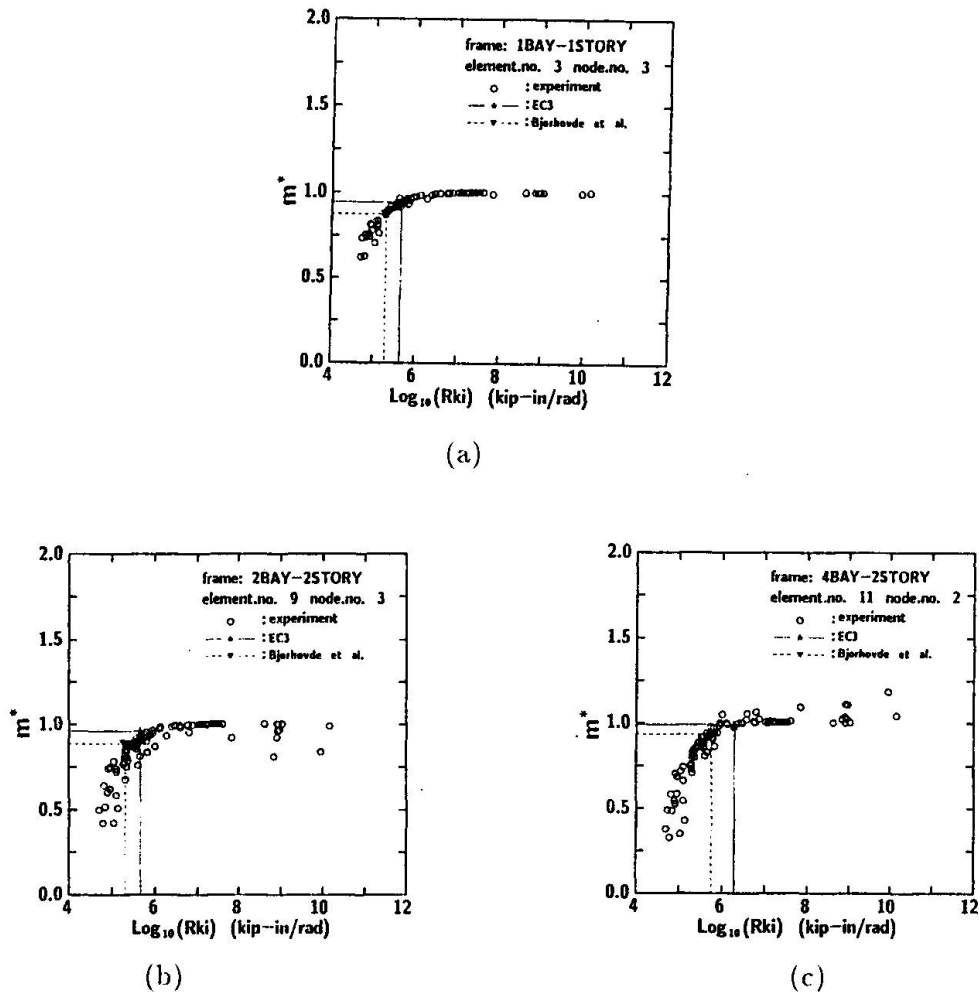


Fig. 5. Beam end moment for extended end-plate connections

5. Discussions on results of frame analysis

5.1 Minimum initial connection stiffness of a rigid connection

Three illustrative examples of $m^* - \log_{10} R_{ki}$ for the three frames are shown in Figs 5(a)~(c). Figures 5a, b, and c show the distributions for node 3 of element 3 (one-bay one-story frame), node 3 of element 9 (two-bay two-story frame) and node 2 of element 11 (four-bay two-story), respectively. One most distinct observation can be made from the $m^* - \log_{10} R_{ki}$ distribution is that: almost all data are clustered in the

vicinity of $m^* = 1$ when their $\text{Log}_{10} R_{ki} \geq 6$. This observation is found valid for all cases (i.e., for all nodes of all frames analyzed). Therefore, this leads to a general conclusion that: the minimum initial connection stiffness R_{ki} for a rigid connection can be assumed to be 10^6 kip-inch/radian. Again, this observation will be found equally valid for drift calculation i.e., $d^* = 1$ when $\text{Log}_{10} R_{ki} \geq 6$ (refer examples in Figs 6a~c). This, therefore, substantiate the previous conclusion. A detail discussion regarding this general conclusion can be found in Hasan et al. (1995).

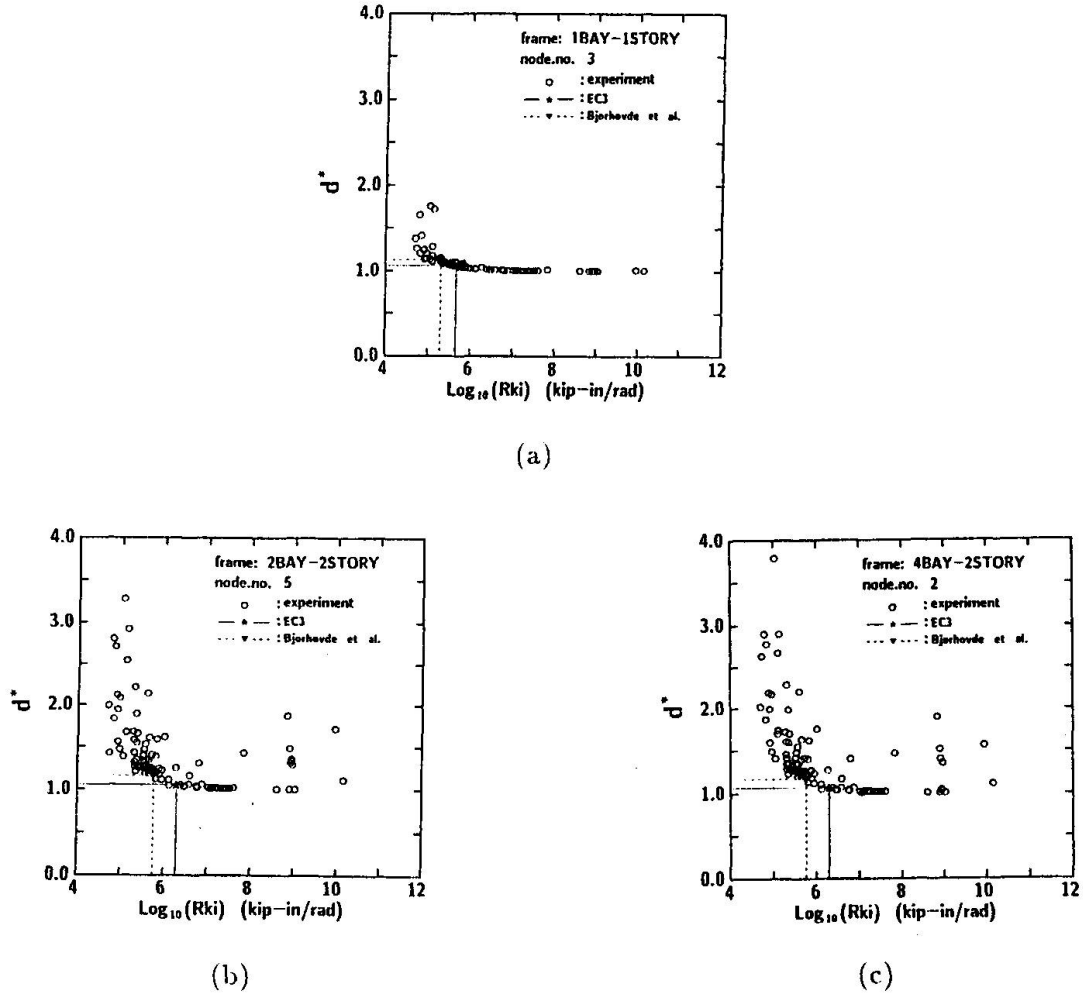


Fig. 6. Frame drift for extended end-plate connections

Table 2. R_{ki} and m^* in the illustrative examples (Figs. 5a~c) for moment analysis

Frame Type	Node	Beam	Min. R_{ki} of a rigid conn. in kip-in/rad.			m^*	
			Present study	EC3	Bjorh.	EC3	Bjorh.
1-bay 1-story	3	W14×22	1.0×10^6	0.48×10^6	0.21×10^6	0.941	0.873
2-bay 2-story	3	W14×22		0.48×10^6	0.21×10^6	0.957	0.884
4-bay 2-story	2	W21×44		2.04×10^6	0.59×10^6	0.987	0.930

The initial connection stiffness and normalized moment in the three examples shown in Figs 5(a~c) are listed in Table 2. The boundary values of initial connection stiffnesses for the roof beam (W14×22) and the floor beam (W21×44) are largely different e.g., 0.48×10^6 kip-in./rad. and 2.04×10^6 kip-in./rad., respectively, as per the



EC3 classification system. This obviously, exposes the inconsistency of the classification systems. The normalized moments correspond to the EC3 classification system are 0.941, 0.957 and 0.987, while their counter-figures for Bjorhovde et al.'s classification system are 0.873, 0.884 and 0.930 for the one-bay one-story, two-bay two-story and four-bay two-story frames, respectively. Therefore, with reference to the normalized moment, both systems of connection classification give conservative results, particularly, Bjorhovde et al.'s classification system.

The numerical values of the initial connection stiffness and normalized drift correspond to the EC3 and Bjorhovde et al.'s classification systems of the three examples in Figs 6(a~c) are tabulated in Table 3. As evident in these three examples, normalized drifts are somewhat equal to unity, however, the EC3 connection classification system performs better than Bjorhovde et al.'s classification system.

Table 3. R_{ki} and d^* in the illustrative examples (Figs. 6a~c) for drift analysis

Frame Type	Node	Beam	Min. R_{ki} of a rigid conn. in kip-in/rad.			d^*	
			Present study	EC3	Bjorh.	EC3	Bjorh.
1-bay 1-story	3	W14×22	1.0×10^6	0.48×10^6	0.21×10^6	1.058	1.125
2-bay 2-story	5	W21×44		2.04×10^6	0.59×10^6	1.046	1.152
4-bay 2-story	2	W21×44		2.04×10^6	0.59×10^6	1.057	1.161

5.2 Maximum initial connection stiffness of a flexible connection

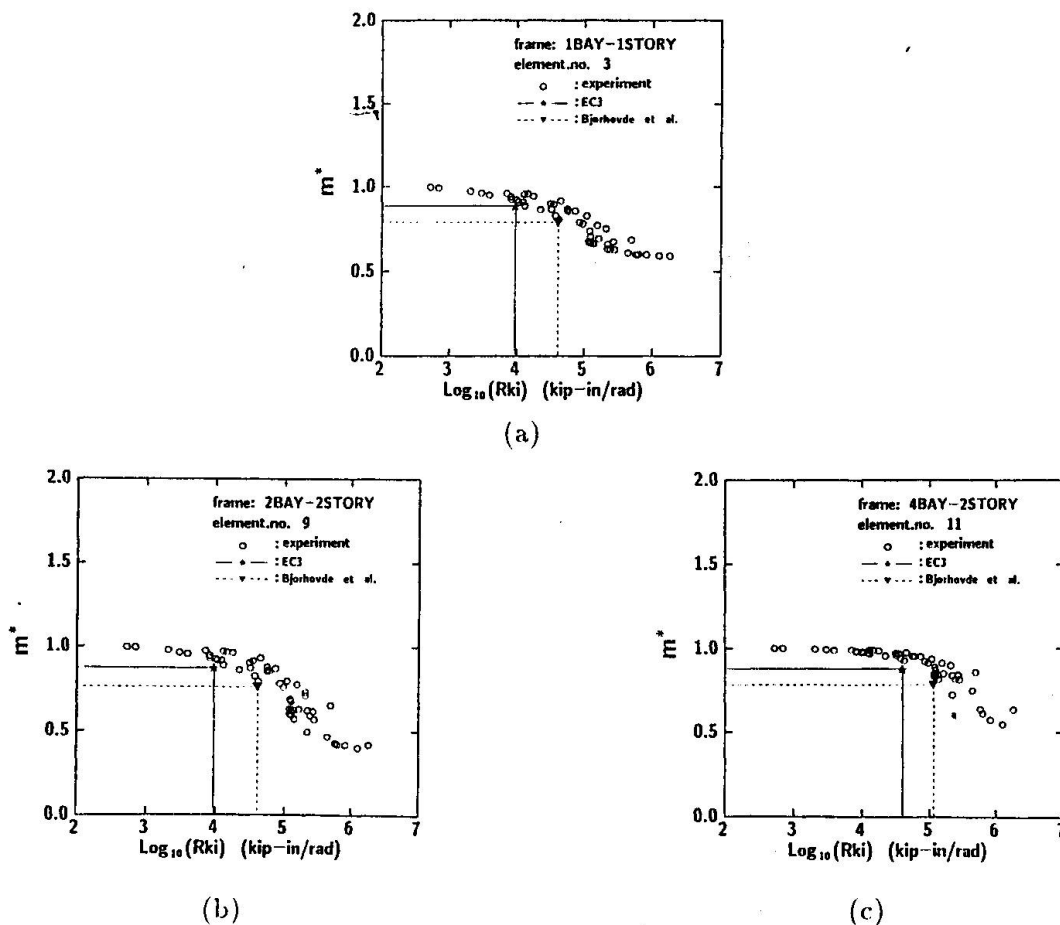


Fig. 7. Beam mid-span moment for single web angle & single plate connections



Figures 7(a)~(c) and 8(a)~(c) show examples of $m^* - \text{Log}_{10}R_{ki}$ and $d^* - \text{Log}_{10}R_{ki}$ distributions, respectively, obtained from frame analysis for the three frames. It is evident from the distribution pattern in these six figures that all data are closely clustered in the vicinity of $m^*=1.0$ or $d^*=1.0$ lines when their $\text{Log}_{10}R_{ki} \leq 4.5$. In other words, the maximum initial connection stiffness of a flexible connection can be regarded as $10^{4.5}$ kip-inch/rad. Again, likewise to rigid connection analysis, this very distinct nature of distribution is found valid for all cases.

The numerical results of the Figs 7 and 8 are listed in Tables 4 and 5. The invalidity of the classification systems are obvious from these results. While frame analysis reveals that the maximum initial connection stiffness of a flexible connection is $10^{4.5}$ kip-inch/rad., the corresponding value as per classification systems vary depending upon the type of the connecting beam (0.96×10^4 , 0.41×10^5 kip-inch/rad. for roof and floor beams, respectively as per the EC3 classification system; and 0.42×10^5 , 0.12×10^6 kip-inch/rad. for roof and floor beams, respectively as per Bjorhovde et al's classification system).

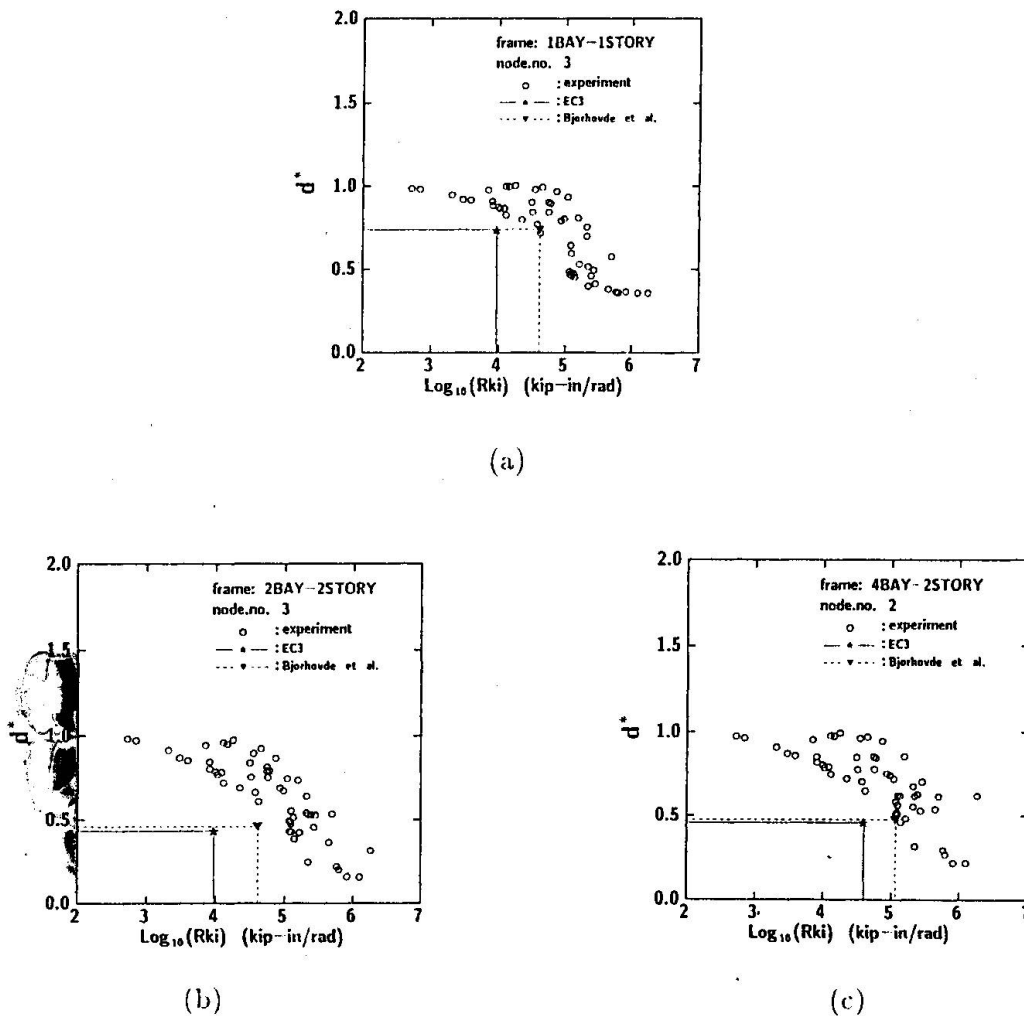


Fig. 8. Frame drift for single web angle & single plate connections

The numerical values of normalized moments m^* and normalized drifts d^* in all cases remain far below 1.0, which provides a cautious indication of unconservative design. Besides, the very low normalized frame responses, particularly for d^* (around 0.4 both for the EC3 and Bjorhovde et al.'s classification systems), raise the question of



the accuracy of demarcation line between semi-rigid and flexible zone with reference to both stiffness and strength.

Table 4. R_{ki} and m^* in the illustrative examples (Figs. 7(a~c)) for moment analyses

Frame Type	Elem.	Beam	Max. R_{ki} of a flexible conn. in kip-in/rad.			m^*	
			Present study	EC3	Bjorh.	EC3	Bjorh.
1-bay 1-story	3	W14×22	$1.0 \times 10^{4.5}$	0.96×10^4	0.42×10^5	0.882	0.758
2-bay 2-story	9	W14×22		0.96×10^4	0.42×10^5	0.870	0.758
4-bay 2-story	11	W21×44		0.41×10^5	0.12×10^6	0.873	0.777

Table 5. R_{ki} and d^* in the illustrative examples (Figs. 8a~c) for drift analyses

Frame Type	Node	Beam	Max. R_{ki} of a flexible conn. in kip-in/rad.			d^*	
			Present study	EC3	Bjorh.	EC3	Bjorh.
1-bay 1-story	3	W14×22	$1.0 \times 10^{4.5}$	0.96×10^4	0.42×10^5	0.732	0.735
2-bay 2-story	3	W14×22		0.96×10^4	0.42×10^5	0.428	0.458
4-bay 2-story	2	W21×44		0.41×10^5	0.12×10^6	0.452	0.473

6. Conclusion

The rationale used to devise non-dimensional connection classification systems (EC3, 1992 and Bjorhovde et al., 1990) is that the connection stiffness should be compared with that of the connected beam. The validity of this rationale is critically examined here by performing frame analysis utilizing experimental data with the perspective of real moment-rotation behavior of connections. This analysis reveals that the two classification systems have a total reliance on the properties of connected beam, even though, a rational classification system should reflect the proper role of all major connection components on connection behavior.

7. References

1. AISC (1994). Manual of Steel Construction, Load and Resistance Factor Design, 2nd Edition, American Institute of Steel Construction, Chicago, IL.
2. Bjorhovde, R., Colson, A. and Brozzetti, J. (1990), "Classification System for Beam-to-Column Connections," J. Struct. Div., ASCE, Vol. 116, No. ST11, 3059-3076.
3. EC3 Code (1992), Design of Steel Structures, Part 1.1, European Committee for Standardization, CEN, Brussels.
4. Goto, Y. and Chen, W.F. (1987), "Second-order Elastic Analysis for Frame Design," J. Struct. Div., ASCE, Vol. 113, No. ST7, 1501-1519.
5. Hasan, R., Kishi, N., Chen, W.F. and Komuro, M. (1995), "Evaluation of Rigidity of Extended End-Plate Connections by Utilizing Updated Data Base," Structural Engineering Report No. CE-STR-95-19, School of Civil Engineering, Purdue University, West Lafayette, IN.



CLASSIFICATION SYSTEM FOR ALUMINIUM ALLOY CONNECTIONS

Federico M. MAZZOLANI **Gianfranco DE MATTEIS** **Alberto MANDARA**
Full Professor of Struct. Eng. Civil Engineer, PhD Student Civil Engineer, PhD

Department of Structural Analysis and Design
University of Naples "Federico II" - Naples, ITALY

Summary

The main problems related to the classification of structural joints in metal structures are discussed in this paper. A new, more general approach, specifically conceived for aluminium alloy structures, is presented in order to overcome the typical limits of existing classification systems, mainly concerned with beam-to-column steel joints. It allows for all load cases to be taken into account. The system is based on a new concept of characteristic length, which allows for a direct comparison between the connection and the connected member.

1. Introduction

In the field of codification of aluminium alloy structures the need for a new assessment of the calculation methods for connections is felt, in order to take into account the actual mechanical feature of these materials. As well known, aluminium alloys exhibit a σ - ϵ relationship of round-house type, which can not be interpreted through the classic elastic-perfectly plastic idealisation, commonly adopted for steel, also because the inelastic extension of some alloys is prematurely limited by low values of ultimate strain. In addition, the behaviour of aluminium alloy structures strongly depends on the chemical composition of the material, the fabrication process, as well as on the heat treatment and presence of reduced strength zones due to welding. Looking forward to a future assessment of appropriate procedures for the evaluation of mechanical features of joints (see for example methods for the evaluation of M versus φ relationship), a preliminary stage is necessary, consisting of a new classification system for connections. This represents a basic tool to establish whether a given joint must be specifically considered into the global analysis of a structure or can be ignored, depending on its mechanical features. In fact, according to the recent knowledge, a joint may be also considered as a sort of "structural imperfection" [1], making the structure under consideration different with respect to the ideal fully rigid or fully pinned scheme. For this reason, it is of prime importance to determine to what extent the disturbance introduced by the joint may be disregarded in the structural analysis and, on the contrary, in what cases it has to be suitably taken into account with appropriate behavioural models. This aspect has been also discussed within the activity of the CEN-TC250/SC9 Committee chaired by Prof. F.M. Mazzolani, which is working out the first edition of Eurocode 9 "Aluminium Alloy Structures" [2]. A general agreement on the opportunity to improve existing approaches to the classification of connections has been reached by all countries.



2. General Requirements for a Classification System

In spite of its importance, in the field of structural analysis, the problem of predicting the actual behaviour of joints is not yet thoroughly solved. In practice, in order to perform an accurate analysis of the structure, the main objective would be that to establish an useful criterion to classify connections as pinned or rigid, in such a way their existence may be disregarded in the calculation of the structure. Nevertheless, it is well known that the actual response of many joints may be neither perfectly pinned nor rigid and that the joint semi-rigidity strongly influences the structural behaviour of the whole system, affecting the overall deformability as well as the load carrying capacity. In these cases, a proper design of the structure should be therefore based on the actual load versus displacement characteristic of the joints. The structural system should be consequently considered as semi-continuous, taking account for the structural properties of connections in terms of strength, stiffness and deformation capacity.

The analysis of a structure should be performed by following the three fundamental steps:

- Classification of connections by checking their properties in terms of stiffness (rigid , semirigid, pinned), strength (full strength or partial strength) and deformation capacity (ductile, semi-ductile, brittle);
- Representation of the load-displacement curve of the joint in a suitable analytical form (this step is skipped in the case of fully restoring joints);
- Modelling and analysis of the structure.

The aim of a classification system is just to define appropriate behavioural classes as a function of the properties of the connected members. This turns to be important also at the light of the method adopted for structural analysis. The assumption made in the global analysis of the structure shall in fact be consistent with the actual behaviour of the joints. For example, in case of linear elastic analysis the classification must be essentially referred to initial rigidity only and a semirigid connection can be modelled by a simple elastic spring, whose elastic constant represents the connection stiffness. Similarly, in the application of plastic design, relying on the assumption of rigid-plastic behaviour of the joints, the connections must be mainly classified referring to strength (see Section 5). Particular cautions should be adopted when a reduced joint deformation capacity is available. In this case, full strength connections should be provided with an extra reserve of resistance in order to cover possible overstrength effects in the members. On the contrary, if the connection has a design resistance less than the connected member one, a sufficient deformation capacity is always required in order to allow for the plastic mechanism to be developed.

Apart from the above considerations, at the light of practical applications, a quantitative criterion as basis of the joint classification is needed. It must provide the boundaries of the behavioural ranges as well as adequate criteria for comparing the connection properties with those of connected members.

3. Consideration on Existing Classification Systems

In the field of steel structures, different joint classification systems have been proposed in technical literature referring to moment resisting frames [3]. It should be pointed out that the term "joint" is generally defined as the part of the structure which transfers the internal forces from one member to another one, including the connection itself, represented by the mechanical fastening system, and the interaction zone between members.

According to EC3 [4], the beam-to-column joints are classified as pinned, semirigid or rigid, depending on the ratio of the connection initial rotational stiffness to the bending stiffness of the connected member. By assuming the whole length of the connected beam as the relevant parameter for the evaluation of member stiffness, the following boundary limits are defined:

- nominally pinned for $\bar{k} \leq 0.5$
- semirigid for $0.5 < \bar{k} < \bar{k}^*$
- rigid for $\bar{k} \geq \bar{k}^*$

where \bar{k} is a non-dimensional stiffness parameter given by $\bar{k} = k_i L / EI_b$, k_i being the initial rotational stiffness of the connection and I_b , L the moment of inertia and the length of the connected beam, respectively. The value of the parameter \bar{k}^* is equal to 8 or 25 for braced and unbraced frames, respectively. These values have been fitted in such a way that the critical elastic multiplier of the vertical loads does not reduce more than 5% when the actual joint rigidity is considered instead of a fully rigid behaviour. This means that only when the effect of joint actual stiffness is negligible on the frame global response, EC3 provision allows for the joint existence to be disregarded in the frame analysis.

With reference to the flexural resistance, the beam-to-column connections are classified as:

- nominally pinned for $\bar{m} \leq 0.25$
- partial strength for $0.25 < \bar{m} < 1$
- full strength for $\bar{m} \geq 1$

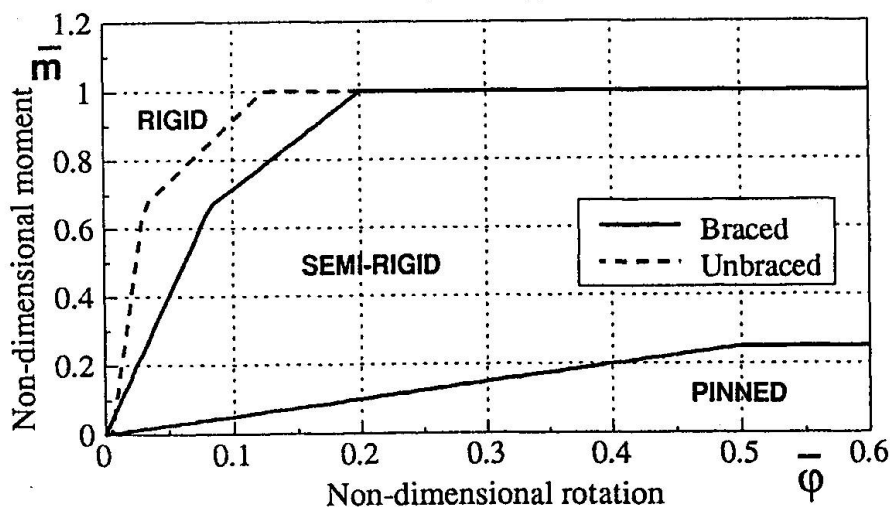


Fig. 1. Connection classification according to Eurocode 3.



\bar{m} being a non-dimensional strength parameter given by $\bar{m} = M_u / M_{pb}$, in which M_u is the peak value of the design moment versus rotation curve of the connection and M_{pb} is the plastic resistance moment of the connected beam. In addition, the control of rotation capacity is not necessary for full strength connections having $\bar{m} \geq 1.2$.

The range of semirigid and rigid connections are bounded by means of a three-linear curve in the $(\bar{m}, \bar{\varphi})$ plane, where the non-dimensional rotation is defined as $\bar{\varphi} = \varphi (EI_b / M_{pb} L)$. The first branch stands up to the value $\bar{m} = 2/3$ for both braced and unbraced frames, whereas the horizontal one starts from a value of $\bar{\varphi} = 0.12$ for unbraced frames and of $\bar{\varphi} = 0.20$ for braced frames (Fig. 1). The boundary curve between semirigid and pinned connections is defined by means of a bi-linear curve. For both braced and unbraced frames, the second branch, which corresponds to the horizontal plateau, starts from the values $\bar{m} = 0.25$ and $\bar{\varphi} = 0.50$ (Fig. 1).

The EC3 classification is based upon the effect of connection on the global response of the frame and is dependent on the length of the connected beam. A different method of classification, which allows to compare directly the connection rotation and the beam curvature, has been proposed by Bjorhovde, Colson and Brozzetti [5]. Such a method is based on the concept of equivalent reference length, assumed as the length L_e of the connected beam whose flexural stiffness EI_b/L_e is equal to the initial rotational stiffness of the connection. On the base of experimental data, the limits of connection stiffness, for both braced and unbraced frames, have been fixed equal to $L_e = 2d$ and $L_e = 10d$ (d is the depth of the beam) in case of rigid-to-semirigid and semirigid-to-flexible connections, respectively. With regard to the ultimate strength, the Authors suggest moment values of $0,7 M_p$ and $0,2 M_p$ for rigid-to-semirigid and semirigid-to-flexible limits, respectively.

Other classification systems, which are independent of the beam length, have been proposed in [6] and [7]. Bijlaard and Steenhuis [6] propose a method based on the same approach of EC3, but with a constant ratio between length and depth of the connected beam ($L/d=25$ for unbraced and $L/d=20$ for braced frames). In the same way, Tschemmerneegg and Huter [7] suggest a classification system in which the distinction between braced and unbraced system is

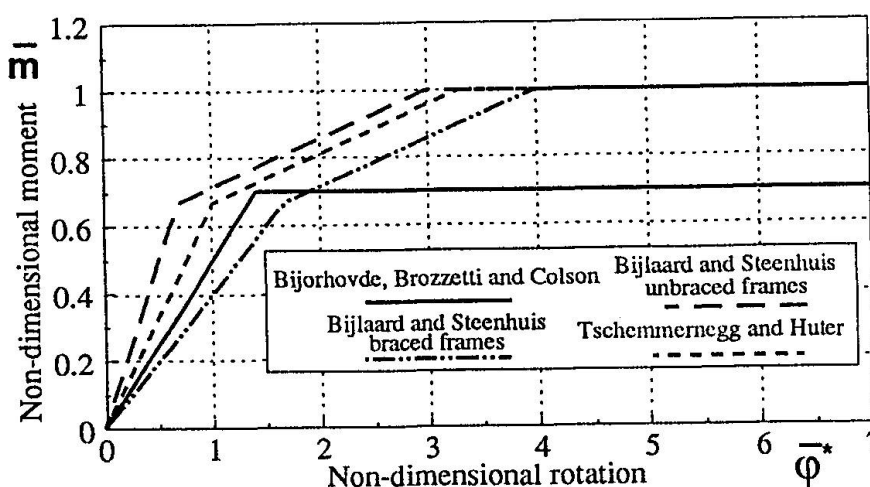


Fig. 2. Boundary curves for different classification systems.

eliminated. In this case the L/d ratio is assumed to vary in such a way to comply with the EC3 joint behavioural limits. A comparison among the above mentioned approaches is depicted in Fig. 2. In this case the non-dimensional rotation parameter has been assumed as

$$\bar{\varphi}^* = \varphi(EI_b/M_{pb}d).$$

4. Needs for a Wider Generality

All the classification systems referred to in the previous paragraph, as well as that proposed in EC3, are mainly concerned with beam-to-column connections. In addition, they account for initial stiffness and ultimate strength separately, without considering the problem of ductility and without taking into account the global behaviour of the connection. For this reason, the existing criteria classify the connections with regard to rigidity or strength independently of each other. Besides, they mostly apply to moment resisting frames, where the moment versus curvature relationship represents indeed the most relevant parameter of the structural behaviour, in particular as far as the global structural response in terms of stability and strength is concerned. This appears as a logical consequence of the wide use of steel moment resisting frames in the current practice. Nevertheless, a need for a more comprehensive approach to the classification of connections is felt, in order to cover also the remaining load cases, namely axial load and shear. This generalisation turns to be particularly suitable in the field of aluminium alloy structures. In fact, in this case, moment resisting frames seldom occur in practice, whereas trussed structures, whose members predominantly work in axial load, can be more frequently used.

On the other hand, some important differences between steel and aluminium alloys also stand from the mechanical point of view, the post-elastic behaviour of aluminium alloys being characterised by peculiar aspects, such as the strain hardening of the material and the available ductility. These aspects can not be ignored in the evaluation of ultimate load bearing capacity of the structure [8], because the strain hardening can produce some unexpected overstrength, whereas the reduced ductility can result in a limitation to the full development of the predicted collapse mechanism. In addition, it is to be considered that the behaviour of aluminium alloy structures is deeply affected by the chemical composition of the material, the fabrication process (extrusion and successive straightening), heat treatment and presence of reduced strength zones due to welding. As a consequence, the analytical computation of the joint response strongly suffers this drastic increment in the number of variables, also by considering the possibility to combine different aluminium alloys for each joint basic component.

This is the main reason why a proposal for a more general classification system is presented in this paper. For this purpose the definitions of generalised force and generalised displacement are introduced, so to cover also cases different from the common moment-rotation relationship. These two parameters account for any possible load-deformation combination. At the same time, a different concept of characteristic length is set up in order to simplify the classification of joint behaviour with respect to the connected member properties. This approach has been shared also within the EC9 Committee, which introduced the classification proposed herein into the chapter 6.4 "Classification of Aluminium Alloy Connections" of the first edition of EC9 [2].



5. A Proposal for a Classification System for Aluminium Alloy Connections

The classification system proposed herein is basically concerned with connections instead of joints. It has been conceived in such a way to achieve a wider generality with regard to the internal actions accounted for as well as the evaluation of joint mechanical features. In fact, this classification applies to all connection typologies subjected to whichever load condition. This has been thought in order to overcome the conventional classification systems for steel connections, which are strictly related to beam-to-column joints, subjected to bending moment. In addition, all mechanical features, namely initial stiffness, ultimate strength and deformation capacity, are involved all at once in the assessment of joint behaviour.

The joint is basically classified according to its capability to restore each one of above properties referred to the connected member. In this way the joint is considered as a sort of imperfection, which must be taken into account in the global structural analysis when it is not able to guarantee the same structural features of the members it connects. This can be considered as an application of the concept of the "industrial frame" according to which also the semirigid behaviour of the joint is interpreted as a "structural imperfection" [1]. The criterion under consideration is based only on the ratio of the properties of the connected

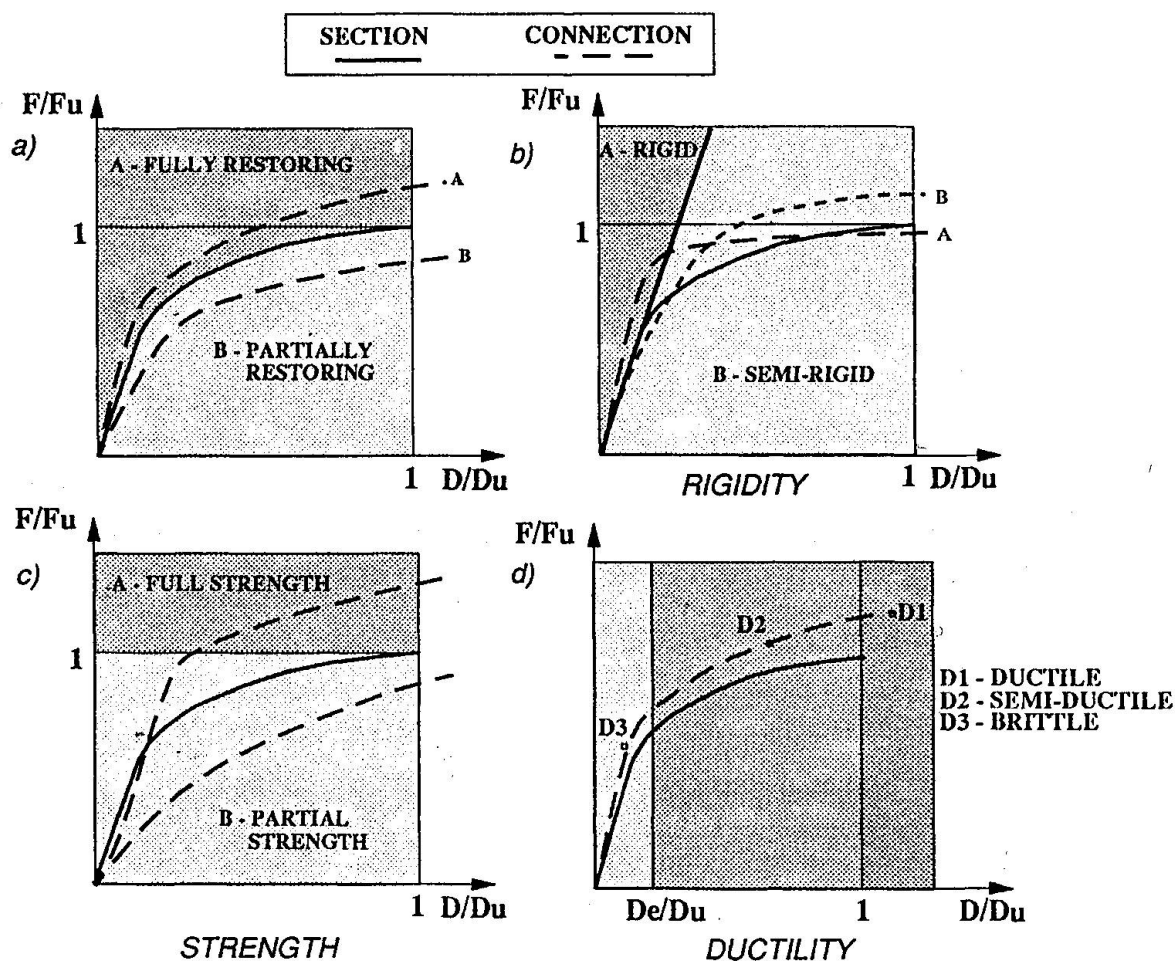


Fig. 3. Connection behavioural classes.

member to those of the connection. Therefore, it is independent of the overall structural response and in particular of the length of the connected members. At the same time, no distinction is made between braced and unbraced frames.

As being stated, the connections may be divided into two fundamental classes (Fig. 3a):

- Fully restoring connections;
- Partially restoring connections.

The former are designed in such a way to have all behavioural properties not lower than those of the weakest connected members. In this case, the existence of the connection may be ignored, regardless of the method of global analysis adopted.

In addition, the restoring features of the connection can be also referred singularly to:

- Elastic rigidity;
- Ultimate strength;
- Ductility.

In this way, it is possible to have connections the following types of connections:

- Rigid and semi-rigid depending on the ratio of their elastic stiffness to that of the connected member (Fig. 3b);
- Full strength or partial strength with reference to the member ultimate strength (Fig. 3c);
- Ductile or non-ductile (semi-ductile or brittle) with reference to member ultimate deformation capability (Fig. 3d).

In order to achieve a more generality, in the above figures the parameters of generalised force (F) and displacement (D) have been considered, expressed in non-dimensional form by means of the ultimate generalised force (F_u) and generalised ultimate (D_u) and/or elastic (D_e) generalised displacement of the connected member section.

In partially restoring connections the behavioural properties of the connection do not reach those of the weakest connected member at least with regard to one property (rigidity, strength or ductility). As a consequence of this, specific allowance for connections should be made depending on the type of global structural analysis. The general requirements for each type of analysis are summarised in Tab. 1. As a general rule, the execution of an elastic analysis requires the connection semirigidity to be taken into account. In the same way, in plastic global analysis, ultimate strength and/or ductility must be accounted for as possible weakening sources for the structures. As far as deformation capability is concerned, when partial strength, ductile connections are involved, the elongation or rotation limits of the connection may be ignored in structural analysis. In partial strength, semi-ductile connections, in which the ductility is lower than the connected member one, elongation or rotation limitations must be considered in inelastic analysis. Brittle connections, which have a ductility lower than the elastic limit deformation of the connected member, must be considered in any kind of global analysis by means of an appropriate check.

All the above considerations lead to the conclusion that the restoring properties of a connection are to be defined in such a way that the connection does not represent a weak point within the structure. Therefore, the existence of the connection must be considered in the structural analysis, depending on the property which is not restored.



6 Definition of Characteristic Length

A direct comparison between the generalised deformation of connection and that of the connected member is required for defining the connection restoring capacity in terms of rigidity and ductility. For this reason, it may be convenient to resume the concept of equivalent reference length, already introduced in [5]. In the present proposal, this can be more effectively defined as characteristic length and corresponds to the length of the member section to be considered in the comparison between connection and connected member. The characteristic length L_c can be therefore intended as the part of member which, starting from an ideal continuous structure, is substituted by the insertion of the connection. It is a function of the joint typology as well as of the connection geometry and it is essentially composed of three different parts:

- The connection itself;
- The member section L_b affected by deformation due to concentrated actions;
- The ideal intersection zone in the joint among connected members, if present.

The latter is often represented by the panel zone, which is common in beam-to-column joints. As far as the length L_b is concerned, it can not be determined "a priori", being dependent on

<i>Method of global analysis</i>	<i>Type of connection which must be accounted for</i>	<i>Type of connection which may be ignored</i>
ELASTIC (Linear or Non-linear).	Semi-rigid connections (Full or Partial strength, Ductile or Non-ductile) with or without restoring of member elastic strength; Partial strength connections (Rigid or Semi-rigid, Ductile or Non-ductile) without restoring of member elastic strength.	Fully restoring connections; Rigid connections (Full or Partial strength, Ductile or Non-ductile) with restoring of member elastic strength; Partial strength connections (Rigid, Ductile or Non-ductile) with restoring of member elastic strength.
PLASTIC (Rigid-plastic, Elastic-plastic, Inelastic-plastic).	Partial strength connections (Rigid or Semi-rigid, Ductile or Non-ductile) without restoring of member elastic strength.	Fully restoring connections; Partial strength, Ductile connections (Rigid or Non-ductile) with restoring of member elastic strength; Full strength connections.
HARDENING Rigid-hardening, Elastic-hardening, Generically inelastic)	Partially restoring connections	Fully restoring connections

Tab. 1. General design requirements.

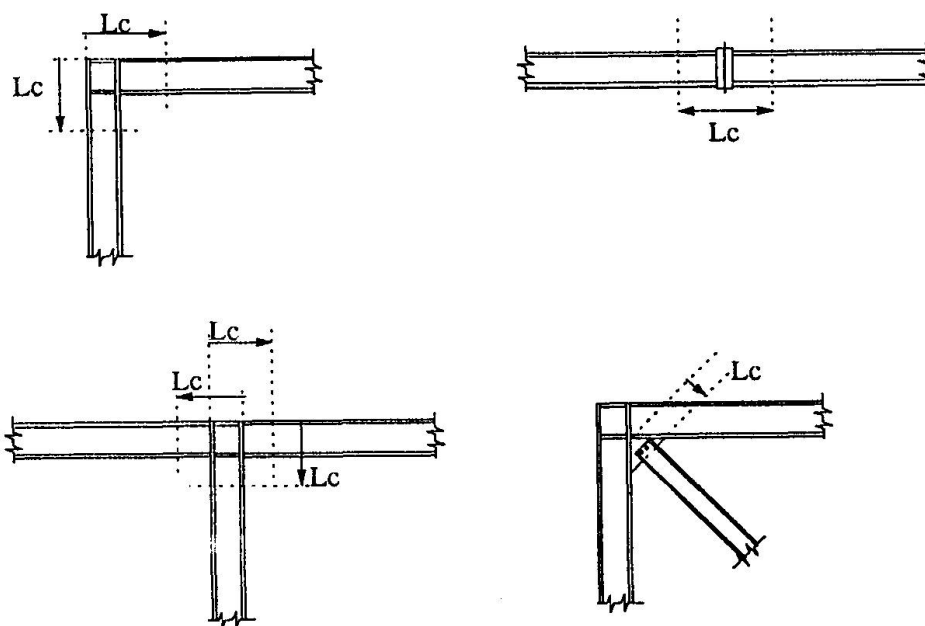


Fig. 4. Characteristic length definition.

both the existing internal action and the deformation mechanism of the joint. In a simplified way, it may be approximately assumed equal to the depth of the member for bending and shear actions and equal to zero for axial actions, unless more reliable evidences do not confirm that more limited or extended member zones are involved in the joint deformation mechanism.

The comparison between the connection and the member in terms of mechanical properties shall be done by referring to each member crossing the joint. For this reason, the value of the characteristic length shall be evaluated for each connection involved into the joint. The representation of characteristic length of the most common connections is reported in Fig. 4 with reference to different kinds of joint. Referring to rigidity and ductility, a connection will be finally defined restoring if its generalised force-displacement relationship is "better" than the one of the connected member, this latter calculated on the base of a member length equal to the characteristic length of the connection. It is also to be emphasised that generalised displacement parameters shall be either a deformation or a curvature, depending on whether axial, shear load or moment is involved.

For example, for a typical beam-to column joint subjected to bending action (Fig. 5a), the comparison in terms of initial rotation can be expressed as follows:

$$\varphi_c \leq \chi(M L_c / E I_b)$$

where, L_c is the characteristic length, M/EI_b is the elastic curvature of the beam for the given bending moment M , and φ_c is the concentrated rotation of the connection under the same bending moment as calculated by means of analytical or experimental procedure. In the application of such procedures, all joint deformation components, elastic and/or plastic, within the zone delimited by the assumed characteristic length, are to be taken into account.

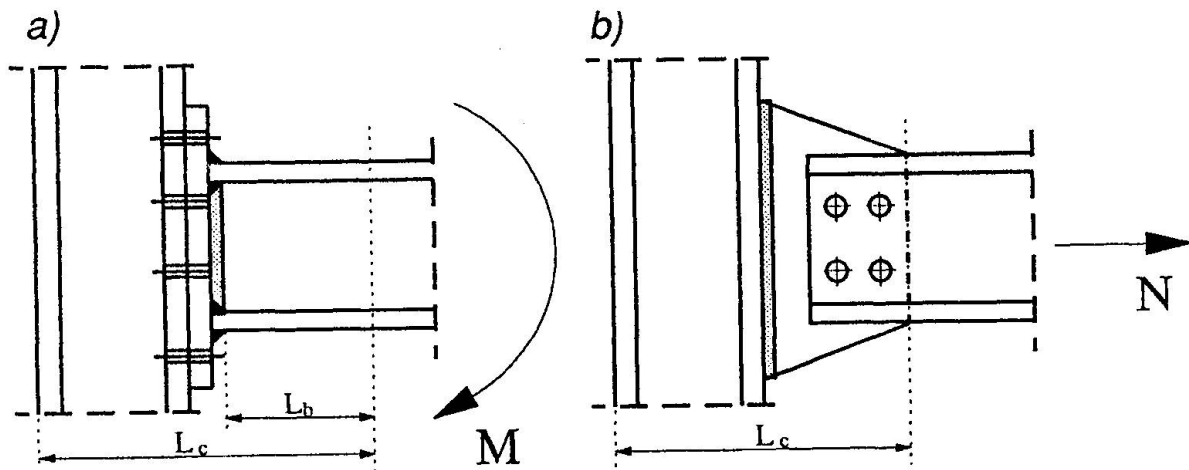


Fig. 5. Characteristic length for bending and axial joints.

Similarly, the assessment of connection axial rigidity may be done through the following inequality (Fig. 5b):

$$\delta_c \leq \chi(NL_c/EA_b)$$

where, L_c is the characteristic length, N/EA_b is the elastic axial deformation of the connected member under the given axial action N , and δ_c is the relative displacement between connected members for the same load.

The coefficient χ is representative of the ratio of connection to member properties which can be accepted to classify the connection as rigid or semirigid. Theoretically, it should be assumed equal to the unit for rigid-to-semirigid limit behaviour, but practically it could be set up on the base of the tolerated effects of joint semirigidity on the behaviour of the structure under consideration. However, it will be never far from the unit value. Similarly, for semirigid-flexible limit behaviour, the χ coefficient must be chosen in such a way that the internal actions as well as the stiffness of connection can be completely disregarded in the structural analysis, with acceptable approximation. At the moment, a suitable approach could be to assume $\chi=0.1\div 0.2$, so that the effects of joint flexibility are neglected if its stiffness is lower than the 10÷20% of that of connected member, these latter referred to the characteristic length.

It is to be pointed out that the assessment of connection rigidity can be done also in inelastic range, and not necessarily in term of initial stiffness, as shown in Fig. 6. In this case, the tangent stiffness of the connected member k_m must be considered in the comparison with connection rigidity k_c .

7 Conclusive Remarks and Further Developments

A new classification system for aluminium alloy connections has been proposed. The main aspects of this classification consist in a new approach for the evaluation of connection properties, as well as in a wider generality in terms of considered internal actions. The method is in fact referred to all internal forces and relative displacements and is applicable to all joint

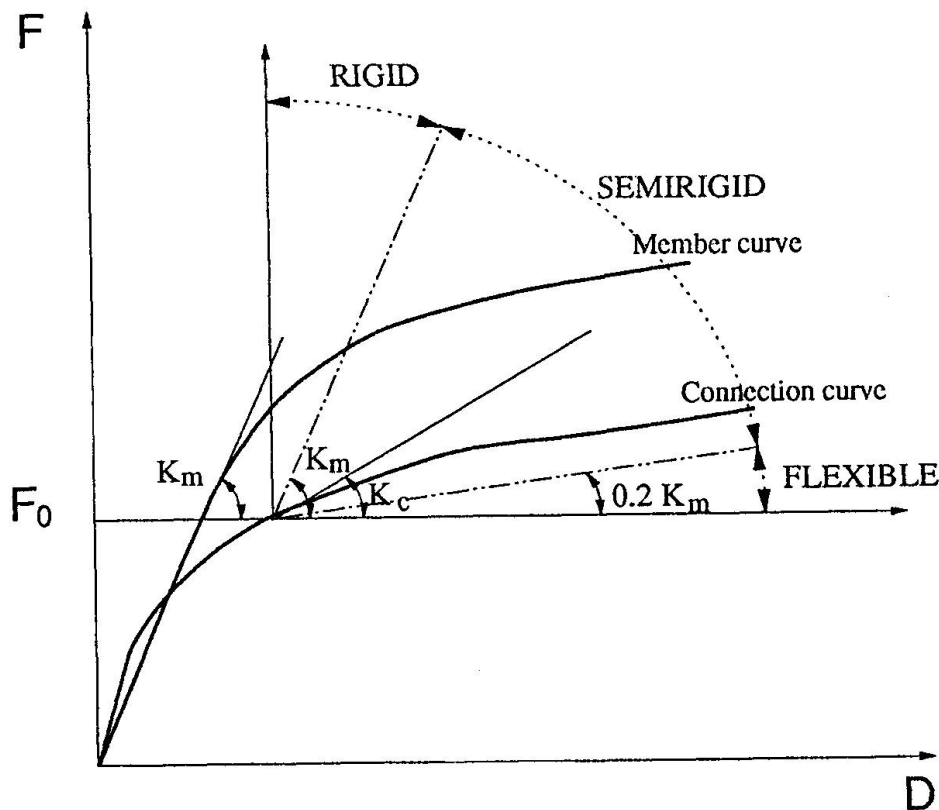


Fig. 6. Connection classification in stiffness.

typologies. In addition, particular attention is paid to the ductility features of the connection, in order to guarantee its capability to accomplish the deformation requirements of a given collapse mechanism.

The joint is classified according to its capability to restore each one of the mechanical properties (initial stiffness, ultimate strength and deformation capacity) of the connected member. Contrary to the EC3 assumptions, which relate the effects of connection to the global behaviour of the structure, the restoring properties are defined on the basis of a local and direct comparison between connection and connected member. In order to allow such a direct comparison, a new concept of member characteristic length has been stated. It represents the length which has to be considered for the evaluation of generalised displacement parameters of the connected member. The characteristic length is a function of the connection geometry and can be thought as the part of the structure affected by deformation arisen as a consequence of the connection. The connection behavioural class limits has been then fixed on the basis of the above mentioned comparison.

The classification presented herein represents the first step of a more general research project, aimed to set up an appropriate guideline for the design of aluminium alloy structures and, in particular, of connections. This effort is framed within the activity of the CEN TC250/SC9 Committee which, under the chairmanship of F.M. Mazzolani, is preparing the first issue of EC9 "Aluminium Alloy Structures", with the contribution of all Countries of the European Union. The next step of this study will be that to improve the calibration of the proposed



approach by means of both experimental and theoretical investigations, devoted to analyse the joint behaviour and the effects of joint semirigidity on the behaviour of the whole structure. The specific allowance for the peculiar features of aluminium alloys is planned to be the basic concern of this research stage, with the expected result to set up a suitable method for evaluating the design moment-rotation characteristic of aluminium alloy joints. For this purpose, an extension of the EC3 method for steel joints is presently being studied, based on the actual non linear behaviour of the material, as well as on the available alloy ductility, which in most cases is lower than in steel. The outcoming of this investigation will contribute to a more effective assessment of this problem in the field of codification, obtained thanks to a more comprehensive approach to both classification of joints and prediction of joint behaviour.

References

- [1] **Mazzolani F.M.**, *Stability of Steel Frames with Semi-Rigid Joints*, CISM Courses and Lectures No. 323: "Stability Problems of Steel Structures", Edited by M. Ivanyi and M. Skaloud, 1992.
- [2] **Commission of the European Communities**: *Eurocode 9: Design of Aluminium Alloy Structures*, 1st Edition, 1996.
- [3] **Mazzolani F.M., Piluso V.**, *Theory and Design of Seismic Resistant Steel Frames*, Chapman and Hall, 1996.
- [4] **Commission of the European Communities**: *Eurocode 3: Design of Steel Structures*, 1994.
- [5] **Bjorhovde R., Brozzetti J., Colson A.**, *Classification System for Beam-to-Column Connections*, Journal of Structural Engineering, ASCE, Vol. 116, N.11, November, 1990.
- [6] **Bijlaard F.S.K., Steenhuis C.M.**, *Prediction of the Influence of Connection Behaviour on the Strength, Deformation and Stability of Frames, by Classification of Connections*, 2nd International Workshop, Pittsburgh, April, 1991.
- [7] **Tschemmermegg F., Huter M.**, *Classification of Beam-to Column Joints*, COST C1 Working Group 2 Meeting, Liege, 14-16 June, 1993.
- [8] **Mazzolani F.M.**, *Aluminium Alloy Structures*, 2nd Edition, E & FN SPON, 1995.



New Classification System for Semi-Rigid Connections Considering Overall Behavior of Frames

Yoshiaki Goto
Professor
Nagoya Institute of Technology
Japan

Yoshiaki Goto, born 1949, got his civil engineering doctoral degree at University of Tokyo. His research interest is in the advanced analysis and design of steel structures. He has been professor at Nagoya Institute of Technology since 1991.

Satoshi Miyashita
Research Associate
Gifu National College of Technology
Japan

Satoshi Miyashita, born 1968, graduated as civil Engineer from Nagoya Institute of Technology. He is engaged in the research on advanced analysis of steel structures. He has been research associate at Gifu National College of Technology since 1993.

A new classification system of semi-rigid connections was proposed. Some typical subassemblages of multistory frames were chosen to consider the layout and member details of the structural systems. The boundary of connections between rigid and semi-rigid was established by taking into account the behaviors of the structural subassemblages at the serviceability limit state along with the ultimate limit state. The validity of the proposed classification system was examined by analyzing the overall behavior of semi-rigid frames.

1. Introduction

It is well known that real beam-to-column connections possess some stiffness that falls between the two extreme cases of fully rigid and ideally pinned. Thus, the modeling of connections as semi-rigid is more realistic. However, in engineering practice some connections can be considered pinned if their stiffness is so small that the connections are incapable of transmitting any significant moment, thus permitting almost free rotation. Similarly, some connections can be considered rigid if their rigidity is so large that no significant slope discontinuity exists between the adjoining members. The assumption of ideally pinned or rigid connections considerably simplifies the design and analysis procedures of framed structures. Thus, it is useful to estimate in advance whether the connections can be assumed rigid, semi-rigid or pinned. Proposals for the classification of connections have been presented by EC3(1992) and Bjorhovde et al(1990). The classification system by Bjorhovde et al. is intended for the case where the prior knowledge concerning the member and structural details is not available. On the other hand, EC3 proposed a classification system based on the load-carrying capacity of frames. This classification is more rational, if the layout and member details of the structural system are known in advance. However, ductility demand is not shown in EC3 classification. This is different from the proposal by Bjorhovde et al. Although EC3 considers the ultimate strength of frames in the classification of connections, it does not take in account the behavior at the serviceability limit



state. Further, in order to evaluate the load-carrying capacity of frames, EC3 adopts an approximate formula, i.e. the Merchant-Rankine formula. The frame model used for this evaluation is also too simple to generally reflect the effect of layout and member details of real frames. In this way, the existing classification systems are still considerably approximate in nature. In fact, a precise elastic-plastic finite-displacement analysis showed that the EC3 boundary between rigid and semi-rigid connections is on the whole considerably restrictive in terms of the ultimate strength of frames(Goto and Miyashita 1995).

In this paper, we will propose a new classification system of connections where the behavior of frames not only at the ultimate limit state but also at the serviceability limit state is considered. The connection model used for the classification is the power model proposed by Kishi et al.(1993). The validity of the proposed classification system is examined by analyzing the elastic-plastic overall behavior of semi-rigid frames.

2. Modeling of Connections

The semi-rigid connections are represented by a discrete, inelastic, rotational spring. The connection model used herein is the three-parameter power model proposed by Kishi et al.(1993). The generalized form of this model is expressed as

$$m = \theta / (1 + \theta^n)^{1/n} \quad (1)$$

where $m = M / M_u$, $\theta = \theta_r / \theta_0$, $\theta_0 = M_u / K_I$,

M = connection moment, M_u = ultimate moment capacity of connection, θ_r = relative rotation between beam and column, K_I = initial connection stiffness and n = shape parameter.

Equation(1) has the shape illustrated in Fig. 1 depending on the value of n . As can be seen from Eq.(1), the connection curve is uniquely determined by three parameters, that is, ultimate moment capacity M_u , initial stiffness K_I and shape parameter n . The formulas to calculate the value of n are determined for several connection types as shown in Table 1, based on statical analysis of test data (Chen and Kishi 1989). The formulas given in Table 1 reduces the independent parameters of Eq.(1) to M_u and K_I . Thus, the classification can be made quantitatively based on these two parameters. That is, the boundary between rigid and semi-

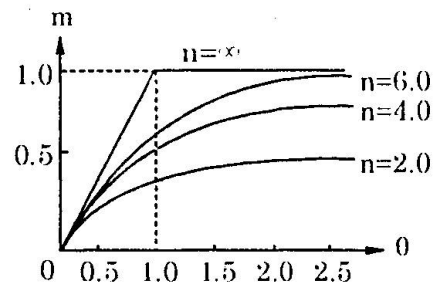


Fig. 1. Three-parameter power model

Table 1. Empirical equation for shape parameter n

Connection Type	n	
Single web-angle connection	$0.520 \log_{10} \theta_0 + 2.291$	$\log_{10} \theta_0 > -3.073$
	0.695	$\log_{10} \theta_0 \leq -3.073$
Double web-angle connection	$1.322 \log_{10} \theta_0 + 3.952$	$\log_{10} \theta_0 > -2.582$
	0.537	$\log_{10} \theta_0 \leq -2.582$
Top-and seat-angle connection (without double web angle)	$2.003 \log_{10} \theta_0 + 6.070$	$\log_{10} \theta_0 > -2.880$
	0.302	$\log_{10} \theta_0 \leq -2.880$
Top-and seat-angle connection (with double web angle)	$1.398 \log_{10} \theta_0 + 4.631$	$\log_{10} \theta_0 > -2.721$
	0.827	$\log_{10} \theta_0 \leq -2.721$

rigid and that between semi-rigid and pinned can be estimated in terms of the values of M_u and K_r . The boundary values for K_r are decided by the behavior of frames at serviceability limit state, whilst those for M_u are determined by the behavior at ultimate limit state.

3. Frame Models

In order to take into account the behavior of frames in the classification of connections, we adopt several subassemblages which will be considered to represent the behaviors of the respective parts of the multistory multibay frames shown in Fig. 2. These subassemblages are chosen by considering the deformation patterns of the respective parts of the sway and non-sway frames illustrated in Fig. 3. The subassemblages so chosen are summarized in Fig. 4. In this figure, it is denoted by the notations $A_s \sim F_s$ and $A_n \sim F_n$ how the respective subassemblages represent the parts of the frames in Fig. 3. For the members of these subassemblages, we consider the linearly distributed residual stress model, initial deflection and the uniaxial constitutive model of material which were presented by Vogel(1984). In this constitutive model, $\sigma_y = 294 \text{ MPa}$ and $E = 2.01 \times 10^5 \text{ MPa}$ are used.

4. Classification of Initial Stiffness K_r of Connection Based on the Behavior of Frames at Serviceability Limit State

4.1 Classification Criteria

Classification of initial connection stiffness will be made by considering the behavior of frames at serviceability limit state. The following criteria defined in terms of displacements is used to classify the semi-rigid connections to be rigid.

$$\Delta_s = (\delta_s - \delta_r) / \delta_r \leq 0.05 \quad (2)$$

where δ_s is a displacement of a frame with semi-rigid connections and δ_r is a displacement of the corresponding rigid frame. The loading conditions used to calculate the displacements are shown in Fig. 4. The loads applied at the serviceability limit state are denoted by V and H. In what follows, the boundary value of the initial stiffness of connections between rigid and semi-rigid will be derived considering the behavior of sway and nonsway frames.

4.2 Sway Frame

The displacements δ_s and δ_r in Eq.(2) are represented by the horizontal displacements at the joint when a horizontal force H is applied to the subassemblages as shown in Fig. 4. In the calculation of δ_s and δ_r , the small displacement theory is applied because the displacements at the serviceability limit state is small. Further, the stiffness of semi-rigid connections is assumed to be linearly elastic. The boundary of the initial connection stiffness between rigid and semi-rigid can be analytically obtained in terms of the nondimensional parameter expressed by

$$\kappa_r^b = (K_r L_c) / (EI_c) \quad (3)$$

The boundaries so obtained for the respective subassemblages are summarized in Table 2(a) where G is a relative stiffness factor defined by

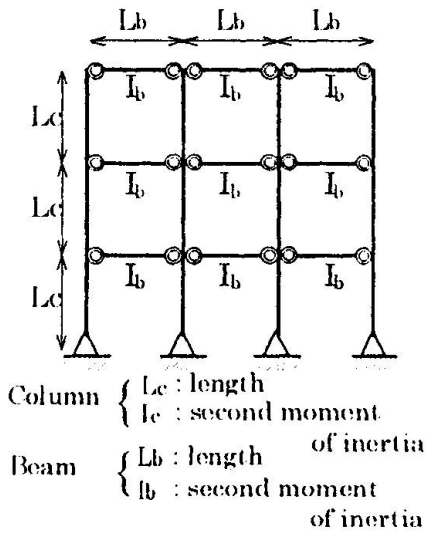


Fig. 2. Multistory and multibay frame

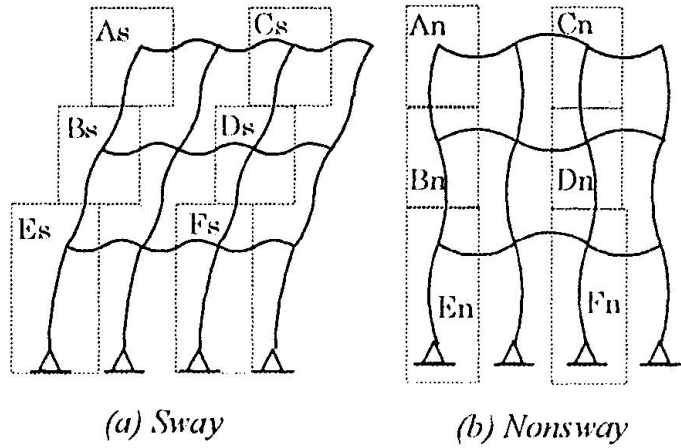
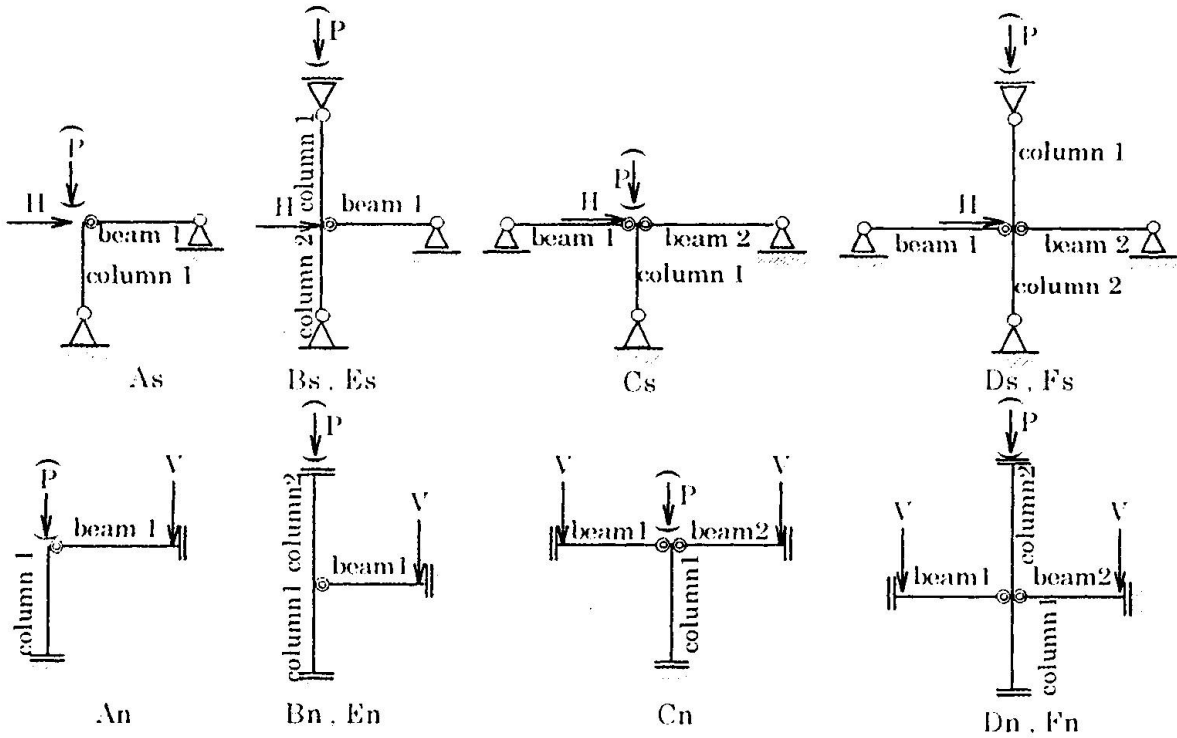


Fig. 3. Deformation pattern of multistory multibay frames



	As, An	Bs, Bn	Cs, Cn	Ds, Dn	Es, En	Fs, Fn
column 1	$L_c/2$	$L_c/2$	$L_c/2$	$L_c/2$	$L_c/2$	L_c
column 2	—	$L_c/2$	—	$L_c/2$	$L_c/2$	$L_c/2$
beam 1	$L_b/2$	$L_b/2$	$L_b/2$	$L_b/2$	$L_b/2$	$L_b/2$
beam 2	—	—	$L_b/2$	$L_b/2$	—	$L_b/2$

V } loads at serviceability
H } limit state
P : loads at ultimate limit state

Remarks ; As ~ Fs , An ~ Fn denotes the parts of multistory multibay frames shown in Fig.3

Fig. 4. Subassemblages

$$G = (I_b / L_b) / (I_c / L_c) \quad (4)$$

EC3 determined the boundary value as $\kappa_i^b = 25$, assuming $G = 1.4$. Therefore, in order to compare our boundary value with that given by EC3, we also show in Table 2(a) the values of κ_i^b when 1.4 is substituted into G . The values of κ_i^b so calculated become either 50 or 31.6, depending on the types of subassemblages. These values are larger than that specified by EC3 as the boundary value between rigid and semi-rigid.

4.3 Nonsway Frame

Similar to sway subassemblages, the boundary of initial connection stiffness between rigid and semi-rigid is determined for nonsway subassemblages based on the criteria expressed by Eq. (2). The displacements δ_s and δ_r in Eq.(2) are represented by the vertical displacements of the beam at the load point when a vertical load V is applied to the beams as illustrated in Fig.4. The boundaries defined in terms of the initial stiffness are shown in Table 2(b) for respective subassemblages. To compare with EC3 classification, the values of κ_i^b with $G = 1.4$ are also shown in Table 2(b). These values which ranges from 11.2 to 29.5 are larger than 8 given by EC3.

Table 2. Boundary value for initial stiffness κ_i^b

(a) Sway Frame		
	κ_i^b	$\kappa_i^b (G = 1.4)$
As, Bs, Cs, Ds	$\kappa_i^b = \frac{6}{(1+G)\Delta}$	50
Es, Fs	$\kappa_i^b = \frac{6(8G+1)}{(4G+3)(3G+1)\Delta} - \frac{6}{3G+1}$	31.6
$\Delta = 0.05$		
(b) Nonsway Frame		
	κ_i^b	$\kappa_i^b (G = 1.4)$
An, Bn	$\kappa_i^b = \frac{6}{(1+G)^2\Delta} - 4$	16.8
Cn, Dn, Fn	$\kappa_i^b = \frac{1}{2} \left(\frac{3}{\Delta} - 1 \right)$	29.5
En	$\kappa_i^b = \frac{6}{(1+G)(1+2G)\Delta} - 2$	11.2
$\Delta = 0.05$		

5. Classification of Ultimate Moment Capacity M_u of Connection Based on the Behavior at Ultimate Limit State of Frames

5.1 Classification Criteria

Classification of ultimate moment capacity M_u of connections is to be made by considering the ultimate behavior of subassemblages. In order to classify the connections to be rigid, EC3 used the following criteria which only considers the ultimate strength of the frames.



$$(P_{ur} - P_{us})/P_{ur} \leq 0.05 \quad (5)$$

where P_{ur}, P_{us} are ultimate strengths, respectively, of rigid and semi-rigid frames.

The criteria expressed by Eq.(5), however, may not be sufficient because the displacement of frames at the ultimate limit state is not reflected. Therefore, we use herein the following classification criteria which takes into account both strength and displacement at the ultimate limit state.

$$\Delta_u = \sqrt{\{(P_{ur} - P_{us})/P_{ur}\}^2 + \{(u_{us} - u_{ur})/u_{ur}\}^2} \leq \sqrt{(0.05)^2 + (0.05)^2} \cong 0.07 \quad (6)$$

where u_{ur}, u_{us} are ultimate displacements, respectively, of rigid and semi-rigid subassemblages. Based on the classification criteria given by Eq.(6), boundaries of ultimate moment capacity of connections between rigid and semi-rigid are determined. The ultimate behaviors of the subassemblages under the load conditions illustrated in Fig.4 are analyzed by the method presented by Goto and Miyashita (1995). This analysis method precisely considers the geometrical and material nonlinearities in the structural response. That is, the geometrical nonlinearity is analyzed by the co-rotational method, whilst the member plastification is taken into account by the plastic-zone method.

5.2 Determine of Boundary Value of Connection Moment Capacity

For the classification of the connection moment capacity, we introduce the nondimensional moment defined by

$$\bar{m}_u = M_u / M_{bp} \quad (7)$$

where M_{bp} denotes the full plastic moment of the connected beam. The connection curve based on the three-parameter power model is governed by the parameter \bar{m}_u . The moment-rotation curves for top- and seat- angle connections with double web angles are illustrated in Fig. 5 with \bar{m}_u ranging from 0.4 to 1.0. The boundary value of \bar{m}_u between rigid and semi-rigid is denoted here by \bar{m}_u^b .

To consider the layout and member characteristics of the subassemblages, two parameters shown below are used.

$$G = \frac{(I_b / L_b)}{(I_c / L_c)}, \quad \lambda = \frac{L_c}{\pi r} \sqrt{\frac{\sigma_y}{E}} \quad (8a,b)$$

where r is the radius of gyration of member cross section. G and λ respectively denote relative stiffness and normalized column slenderness ratio. The ranges of these parameters are determined by considering the layout and member details of practical semi-rigid steel frames.

Taking the sway subassemblage D_s with top- and seat-angle connections with double web angles for an example, the boundary value \bar{m}_u^b between rigid and semi-rigid is to be determined based on the criteria expressed by Eq.(6). The boundary values \bar{m}_u^b obtained for the respective values of the two structural parameters G and λ are shown in Fig. 6. It can be seen from this figure that \bar{m}_u^b becomes large with the increase of λ or G . It should be noted that \bar{m}_u^b exceeds unity for the cases with $\lambda = 1$ or ($\lambda = 0.6, G = 0.7$). This is different either from the EC3 classification where

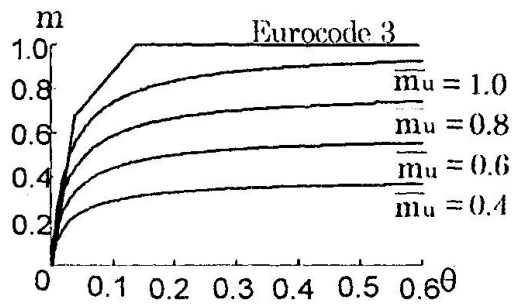


Fig. 5. Moment-rotation curves for top-and seat angle connections with double web angle

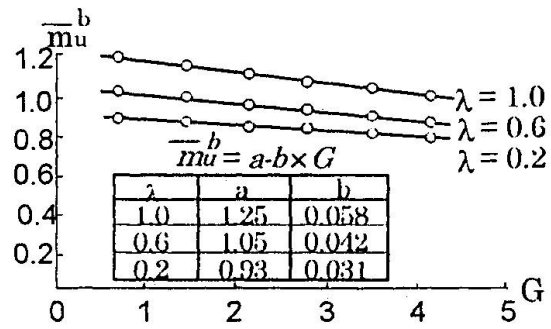


Fig. 6. $\bar{m}_u^b - G$ relation

\bar{m}_u^b is unity or the Bjorhovde classification where \bar{m}_u^b is 0.7. As can be seen from Fig. 6, the relation between \bar{m}_u^b and G can be well approximated by the function in the form

$$\bar{m}_u^b = a - bG \quad (9)$$

where a and b are assumed here to be expressed by the linear functions of λ . These linear functions are determined as follows by the least square method.

$$a = 0.828 + 0.388\lambda \quad b = 0.024 + 0.029\lambda \quad (10a,b)$$

The formula given by Eqs.(9) and (10a,b) coincides well with the numerical results, as compared in Fig. 6.

Following the same procedures as explained above, the boundaries of connection moment capacity \bar{m}_u^b between rigid and semi-rigid are obtained for the rest of the sway and nonsway subassemblages shown in Fig. 4. These subassemblages are assumed to have top- and seat-angle connections with double web angles. Formulas to predict the boundaries of connection moment capacity \bar{m}_u^b are shown in Table 3.

Table 3. Formulas to predict \bar{m}_u^b

	Nonsway subassemblage	Sway subassemblage
A	$\bar{m}_u^b = (1.161 + 0.150\lambda) - (0.026 + 0.005\lambda) \cdot G$	$\bar{m}_u^b = (0.732 + 0.248\lambda) - (0.015 + 0.005\lambda) \cdot G$
B	$\bar{m}_u^b = (0.976 + 0.324\lambda) - (0.027 + 0.011\lambda) \cdot G$	$\bar{m}_u^b = (0.679 + 0.300\lambda) - (0.026 + 0.015\lambda) \cdot G$
C	$\bar{m}_u^b = (0.909 + 0.331\lambda) - (0.027 + 0.019\lambda) \cdot G$	$\bar{m}_u^b = (0.630 + 0.260\lambda) - (0.004 + 0.003\lambda) \cdot G$
D	$\bar{m}_u^b = (0.836 + 0.396\lambda) - (0.024 + 0.031\lambda) \cdot G$	$\bar{m}_u^b = (0.658 + 0.196\lambda) - (0.014 + 0.001\lambda) \cdot G$
E	$\bar{m}_u^b = (0.811 + 0.385\lambda) - (0.029 + 0.004\lambda) \cdot G$	$\bar{m}_u^b = (0.678 + 0.134\lambda) - (0.008 + 0.004\lambda) \cdot G$
F	$\bar{m}_u^b = (0.680 + 0.361\lambda) - (0.019 + 0.024\lambda) \cdot G$	$\bar{m}_u^b = (0.494 + 0.242\lambda) - (0.005) \cdot G$

5.3 Validity of the New Classification System

We shall examine the validity of the aforementioned new classification system of semi-rigid connections, when applied to the multistory and multibay semi-rigid frames. Test frames considered herein consist of two sway frames and two nonsway frames which are illustrated in

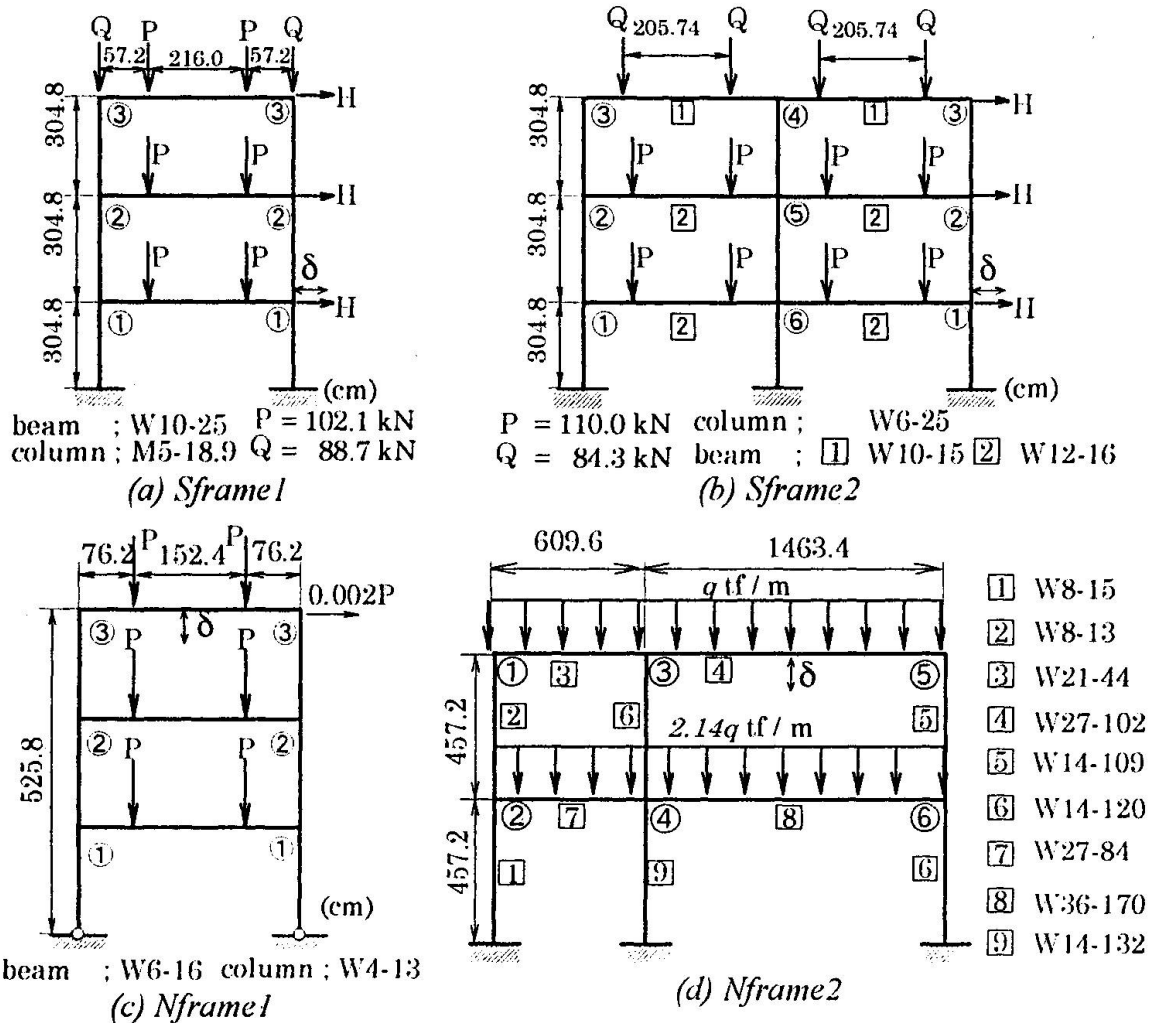


Fig. 7. Test frames

Fig. 7 along with the loading conditions. Sway frames denoted by *Sframe1* and *Sframe2* were shown by Yarimci (1966), while nonsway frames denoted by *Nframe1* and *Nframe2* were respectively designed by McNamee and Lu (1972) and Ziemian (1992). The test frames are assumed to have the top- and seat-angle connections with double web angles with the moment-rotation characteristics which coincide with the proposed boundary between rigid and semi-rigid. The governing parameters for the respective connections are determined from Tables 2 and 3, by considering the layout and details of the connected members. The connection parameters so determined are summarized in Table 4. The validity of the new classification system will be confirmed, if the behavior of the test frames satisfies the criteria expressed by Eqs.(2) and (6) within a reasonable tolerance.

The behavior of the test frames up to the ultimate states is analyzed by the elastic-plastic finite displacement analysis. For *Sframe1* and *Sframe2*, the horizontal force H is monotonically increased with keeping the vertical loads P and Q constant, whilst the vertical load P is monotonically increased for *Nframe1* and *Nframe2*.

As the results of numerical analysis, the load- displacement relations of *Sframe1* and *Nframe1* are shown in Fig. 8. In these figures, we also demonstrate the results where all the connections

Table 4. Boundary values of connection parameters between rigid and semi-rigid

	connection	κ_i^b	m_u^b	subassembly	G	λ
Sframe1	1	10.437	1.071	As	6.477	0.758
	2	16.049	0.993	Bs	6.477	0.758
	3	16.049	1.082	Es	6.477	0.758
Sframe2	1	64.509	0.862	As	0.860	0.586
	2	52.495	0.810	Bs	1.286	0.586
	3	52.495	0.743	Es	1.286	0.586
	4	64.509	0.777	Cs	0.860	0.586
	5	52.495	0.751	Ds	1.286	0.586
	6	52.495	0.629	Fs	1.286	0.586
Nframe1	1	8.638	0.964	En	1.633	0.529
	2	13.309	1.094	Bn	1.633	0.529
	3	13.309	1.194	An	1.633	0.529
Nframe2	1	83.065	1.267	An	0.174	0.739
	2	40.956	1.076	En	0.458	0.725
	3	29.500	1.006	Cn	0.820	0.379
	4	29.500	0.781	Fn	1.280	0.379
	5	28.822	1.193	An	0.912	0.381
	6	4.203	0.885	En	2.370	0.381

are assumed to be rigid. The values of Δ_s and Δ_u defined by Eqs.(2) and (6) for respective test frames are summarized in Table 5. The criteria at serviceability limit state is checked by the load level which is 1/1.4 of the maximum load of the corresponding rigid frame. The value of 1.4 is considered here as a load factor. The value of Δ_s ranges from 0.002 to 0.004, while that of Δ_u ranges from 0.019 to 0.041. All these values of Δ_s and Δ_u satisfy the criteria given by Eqs.(2) and (6). Although all the values of Δ_s are rather small compared with the specified value of 0.05, those of Δ_u are almost comparable to 0.07 specified by the criteria. In order to further examine the validity of the boundary of connection parameters between rigid and semi-rigid, we analyze the behavior of the test frames by decreasing the value of the connection parameter \bar{m}_u from \bar{m}_u^b . In this analysis, the value of κ_i^b is kept constant. We show in Fig. 9 the

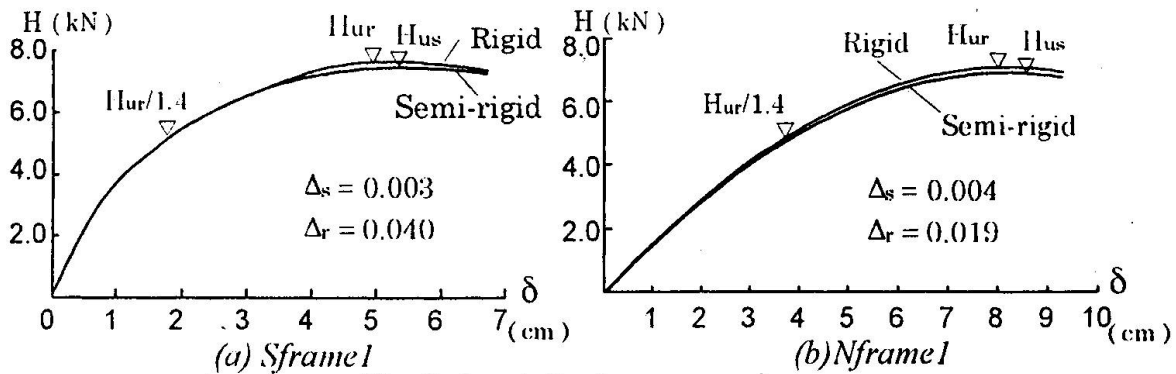


Fig. 8. Load-displacement relations



relation between \bar{m}_u and Δ_u that is calculated based on the ultimate behavior of the respective test frames. It can be seen from this figure that Δ_u approaches the boundary value of 0.07 specified by Eq.(6), when \bar{m}_u is reduced to $0.94 \bar{m}_u^b \sim 0.96 \bar{m}_u^b$. This implies that the proposed boundary values of connection parameters are relatively accurate to classify the connections into rigid and semi-rigid specifically in terms of the ultimate behavior of frames.

6. Summary and Concluding Remarks

A new classification system for semi-rigid connections was proposed. In the new classification system we considered the behavior of semi-rigid frames at the serviceability limit state along with the ultimate limit state. Taking the top- and seat-angle connections with double web angles for an example, we showed a procedure to determine the boundary of connection curves between rigid and semi-rigid. The validity of the new classification system was confirmed by analyzing the elastic-plastic overall behavior of semi-rigid frames. This new classification procedure is also applicable to the other types of semi-rigid connections

Table 5. Values of Δ_s and Δ_r

	Sframe1	Sframe2	Nframe1	Nframe2
Δ_s	0.003	0.004	0.002	0.003
Δ_r	0.040	0.019	0.041	0.039

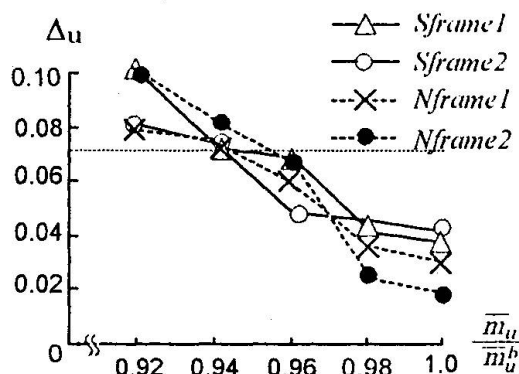


Fig.9. $\Delta_u - \bar{m}_u / \bar{m}_u^b$ relations

7. References

- Bjorhovde ,R., Colson ,A. and Brozzetti , J. (1995) A classification system for beam to column connections , J. Struct. Engng, 116(11) , pp3059-3076, ASCE
- Chen ,W.F and Kishi ,N.(1989) Semi-Rigid Steel Beam-to-Column Connections: Date Base and Modeling , J. Struct. Engng , 115(ST7) , pp.105-119 , ASCE
- Eurocode3 (1990) Design of steel structures: part I - General rules and rules for buildings, Vol.1 Issue 3
- Goto ,Y. and Miyashita,S. (1995) Validity of classification systems of semirigid connections Engineering Structures ,Vol.17 , No.8 , pp544-553
- Kishi ,N. et al.(1993) Design aid of semi-rigid connections for frame analysis , Engineering Journal 3rd quarter , pp90-107 , AISC
- McNamee, B. , M. and Lu ,L.W. (1972) Inelastic Multistory Frame Buckling , Journal of the Structural Division, Vol.98, No.ST7, pp.1613-1631, ASCE
- Vogel , U. (1994) Ultimate limit state calculation of sway frames with rigid joints, ECCS publication 33(first edn) , Rotterdam , ECCS
- Yarimci ,E.(1966) Incremental Inelastic Analysis of Framed Structures and Some Experimental Verifications, Ph.D. Dissertation Dept.of Civil Engineering ,Lehigh University ,Bethlehem ,PA
- Ziemian, R. ,D. (1992) A Verification Study for Methods of Second-Order Inelastic Analysis , Annual Technical Session , Structural Stability Research Council , Pittsburgh , PA



Experimental analysis of semi-rigid composite frames

Fausto Benussi
Associate Professor
University of Trieste
Trieste, Italy

Claudio Bernuzzi
Associate Researcher
University of Trento
Trento, Italy

Salvatore Noè
Associate Researcher
University of Trieste
Trieste, Italy

Riccardo Zandonini
Full Professor
University of Trento
Trento, Italy

Summary

Beam-to-column joints in steel-concrete composite frames generally provide a non negligible degree of flexural continuity, which substantially improves the overall performance of the structural system. The traditional design approaches based on simple frame models thus result inadequate for an "optimal" design of the composite frames. More refined rules should be defined in order to account for the relevant benefits associated with the joint action. This paper summarises an experimental study carried out at both Universities of Trento and Trieste, and presents the first results of the full scale tests on two different steel-concrete composite sub-frames under monotonic loading.

1. Introduction

No sway steel-concrete composite frames are usually designed with reference to the simple frame model, i.e. the composite beams are considered simply supported and the columns resist to the vertical loads and to the bending moments associated with the eccentricity of the beam reactions. This design philosophy neglects the relevant benefits provided by the action of the composite joints, as it is shown by the several experimental and theoretical studies carried out in the past [1]. Also in the case of low amount of longitudinal reinforcement bars in the slab, which in the current practice is used to limit the cracking of the concrete, the composite joints are stiff enough to decrease remarkably the over stressing or the excessive deflections in the beams under working loads. Therefore, significant improvements of the structural behaviour can be obtained by a complete understanding of the nature of the joint action and consequently by an efficient use of the semi-continuity of the frame.

Two different types of flexural continuity are associated with a composite node [2]: (1) the beam-to-beam continuity, due to reinforcing bars, and (2) the beam-to-column continuity, mainly provided by both the steel connection details and the contact between the slab and the column faces. In the past extensive investigations were devoted to the former through a great number of tests on composite joints to internal columns under symmetrical loading conditions, while a very limited series of data on the possible degree of continuity provided by the beam-to-column interaction is presently available. As a consequence, the state of the knowledge does not allow a full understanding of the interaction mechanism between all structural components



in the nodal zone under a general loading condition (i.e., different values of the bending moment in the node due to the presence of composite beams).

A joint study between the Universities of Trento (I), Trieste (I) and Nottingham (UK) was focused on the study of joint action in steel-concrete composite frames [3]. In the framework of this general research project two series of full-scale tests both on composite frames and on composite sub-frames were planned and carried out for obtaining an important basis of knowledge for the complete understanding of the performance of composite connections tested in a frame environment.

In this paper the part of the experimental phase of the research developed by the Italian partnerships is outlined, and the main features of two full-scale tests on steel-concrete composite sub-frames under monotonic loading are presented. A report on the very preliminary findings related to the data analysis phase, which is currently under development, is also presented.

2. The experimental analysis

Two one storey, two bays steel-concrete composite sub-frames were designed, assembled and tested (fig. 1). Beam spans, member sizes and connection detailing were selected in order to satisfy the prime requirement of consistency among the different activities of the general research project [3], i.e. to achieve conditions as close as possible to the frames and limited frames [4] tested at the Building Research Establishment (BRE), also with reference to the main features of the expected response, within the restraints imposed by the testing rig and by the use of European sections.

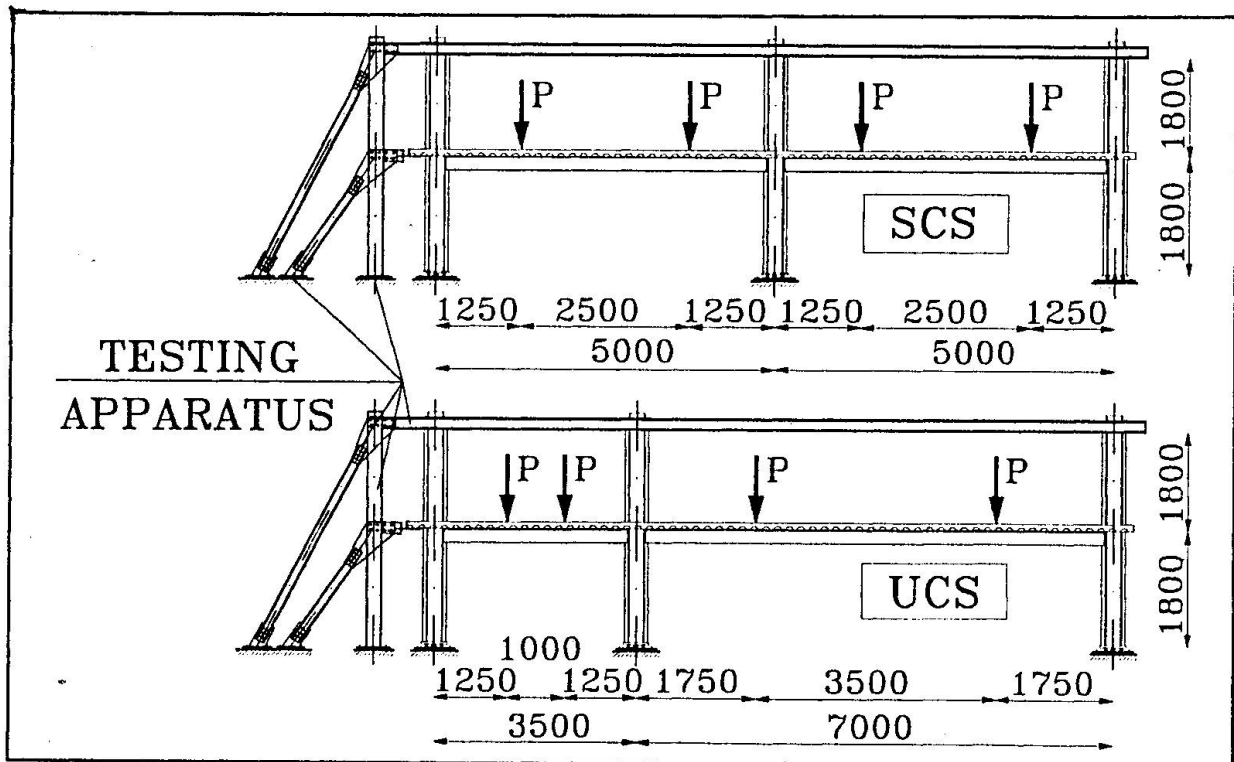


Fig. 1. Composite sub-frame specimens

The design phases of the two sub-frames were carried out according to the rules provided by both Eurocode 3 [5] and Eurocode 4 [6]. The geometrical configuration and the loading pattern of the specimens are presented in fig. 1. The first specimen is characterized by equal 5.0 meters long beam spans (SCS), while in the second one (UCS) the beam span lengths are 3.5 and 7.0 meters respectively. By comparing tests on specimens with symmetrical and unsymmetrical beam spans the effects of the beam-to-beam and beam-to-column continuities provided by composite joints are investigated. For the columns and the steel part of the beams HEB 260 and IPE 240 profiles respectively were selected. The steel beam-to-column connections are flush end plates welded to the steel beams and bolted to the column with 4 M20 bolts grade 8.8 pre-tightened according to the Eurocode 3 criteria (fig. 2).

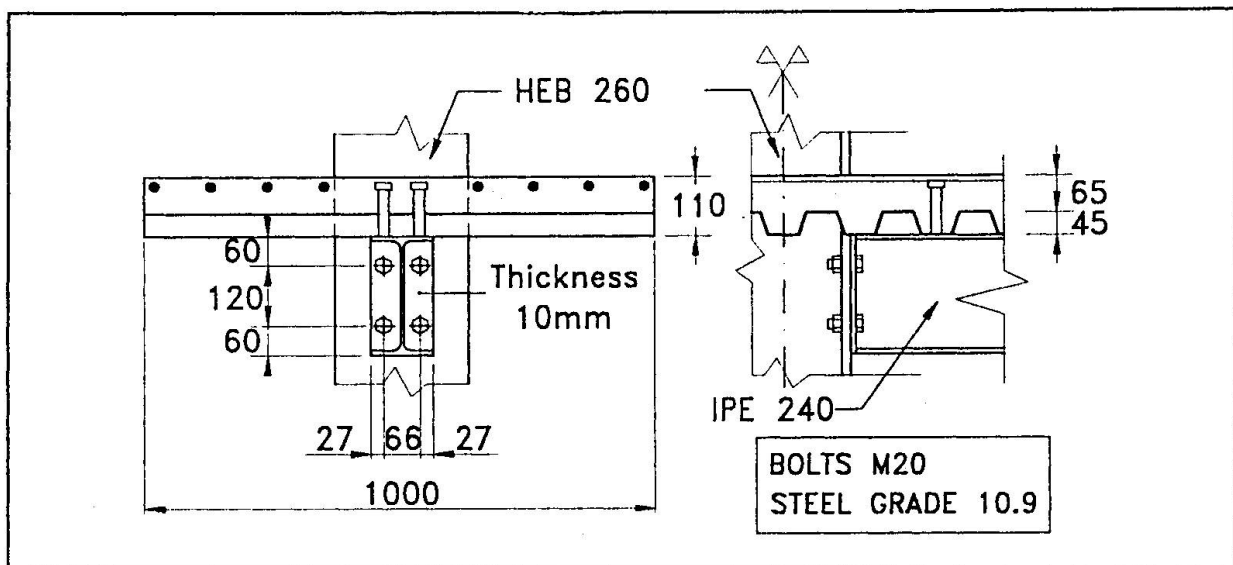


Fig. 2. Composite joint

The composite cross-sections of the beams was designed assuming full interaction between the steel beam and the concrete slab on steel decking with ribs perpendicular to the beam. The slab reinforcing ratio equal to 1.0 % ($8\phi 12\text{mm}$ bars) was selected with reference both to the joint hogging flexural capacity and to the requirements of satisfactory rotational capacity provided through a joint collapse due to the yielding of the rebars. For the external joints, where the problems of anchorage of the longitudinal rebars play a fairly important role, additional trimming bars ($2\phi 16\text{mm}$) were placed in the slab for increasing the structural performance of the node, according to previous studies [7]. The layout of the longitudinal and transverse reinforcing bars is reported in fig. 3. As to the material properties, the mean yield strength values determined through tensile tests were 333 MPa for the steel beam, 292 MPa for the steel column, 463 MPa for the longitudinal rebars and 546 MPa for the additional trimming bars. The concrete of the slab was characterised for the SCS and the UCS sub-frames by a mean value of the cylindrical compressive strength of 51 MPa and 34 MPa respectively. The values of the tensile concrete strength, determined via split-cylinder tests, were 4 MPa and 3 MPa.

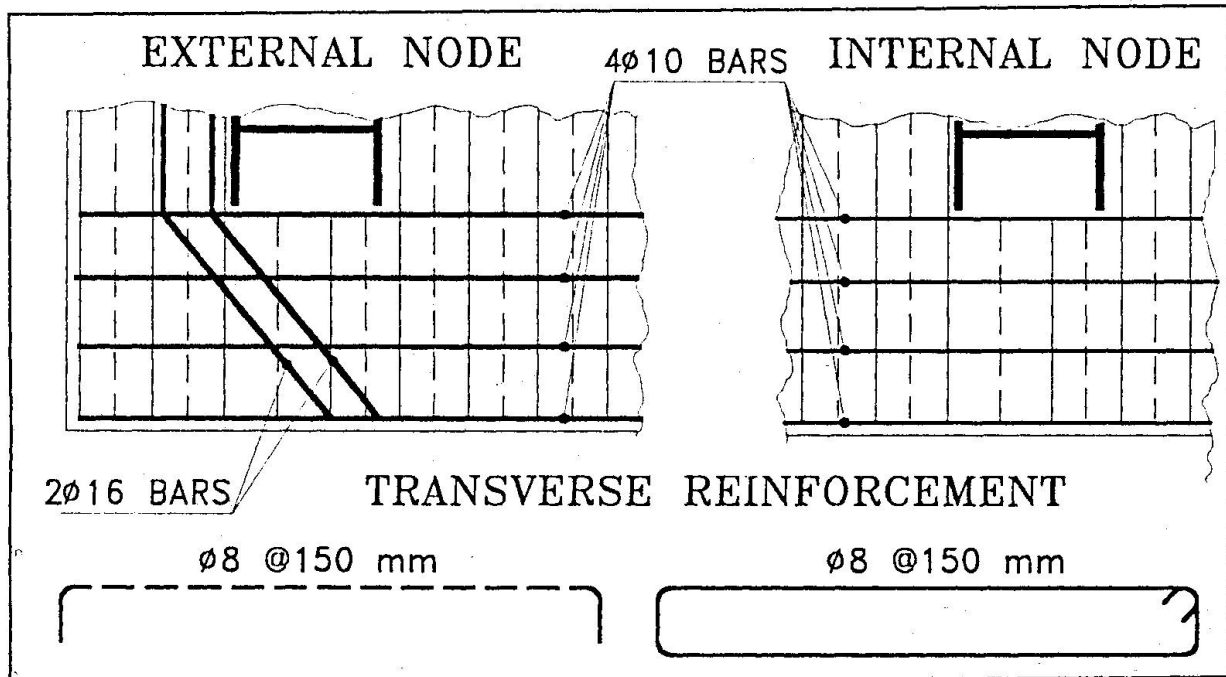


Fig. 3. Slab reinforcement

The measuring system [8] was designed in order to allow the monitoring of both the global response of the tested sub-frames and of the local behaviour of the nodal zones (fig. 4 and fig. 5): inductive transducers (LVDT), electrical strain gages, inclinometers and load cells were used for a total of about 220 measuring points.

The instrumentation system allowed the evaluation of:

- the vertical deflection of the composite beams at different cross sections (LVDTs A);
- the relative rotation of the cross section of the beam at 290mm from the outer face of the column with respect to it (LVDTs B);
- the slip between the concrete slab and the steel beam in the vicinity of the column (LVDTs C);
- the horizontal displacements between the top ends of the columns and the horizontal displacements at the level of the composite beams (LVDTs D);
- the rotation of the web column panel and of the beams in the vicinity of the joints (inclinometers E);

Electrical strain gages were used to monitor the local behaviour of the main relevant components of the sub-frames. Those located on the concrete slab in the vicinity of the nodal zones permitted to analyse the slab performance when the concrete is fully effective. The strain gages located at different sections of the steel beams together with those on the most inner and outer couples of the longitudinal rebars (at the same sections) allowed a refined appraisal of the beam curvature. The internal forces of the column were evaluated by monitoring the strain of the column flanges. As to the nodal zones, the transfer force mechanism was appraised via the readings of the strain gages located at the column web panel and, for joints to external column, also in the additional trimming bars. In the case of UCS sub-frame, the strain gages were connected to the computer assisted data logging system before the phase of concreting of the slab. It permitted an appraisal of the internal forces due to the constructing stage and to the shrinkage of the concrete up to the beginning of the test, which plays an important role in the statically indeterminate structures, such as the sub-frames.

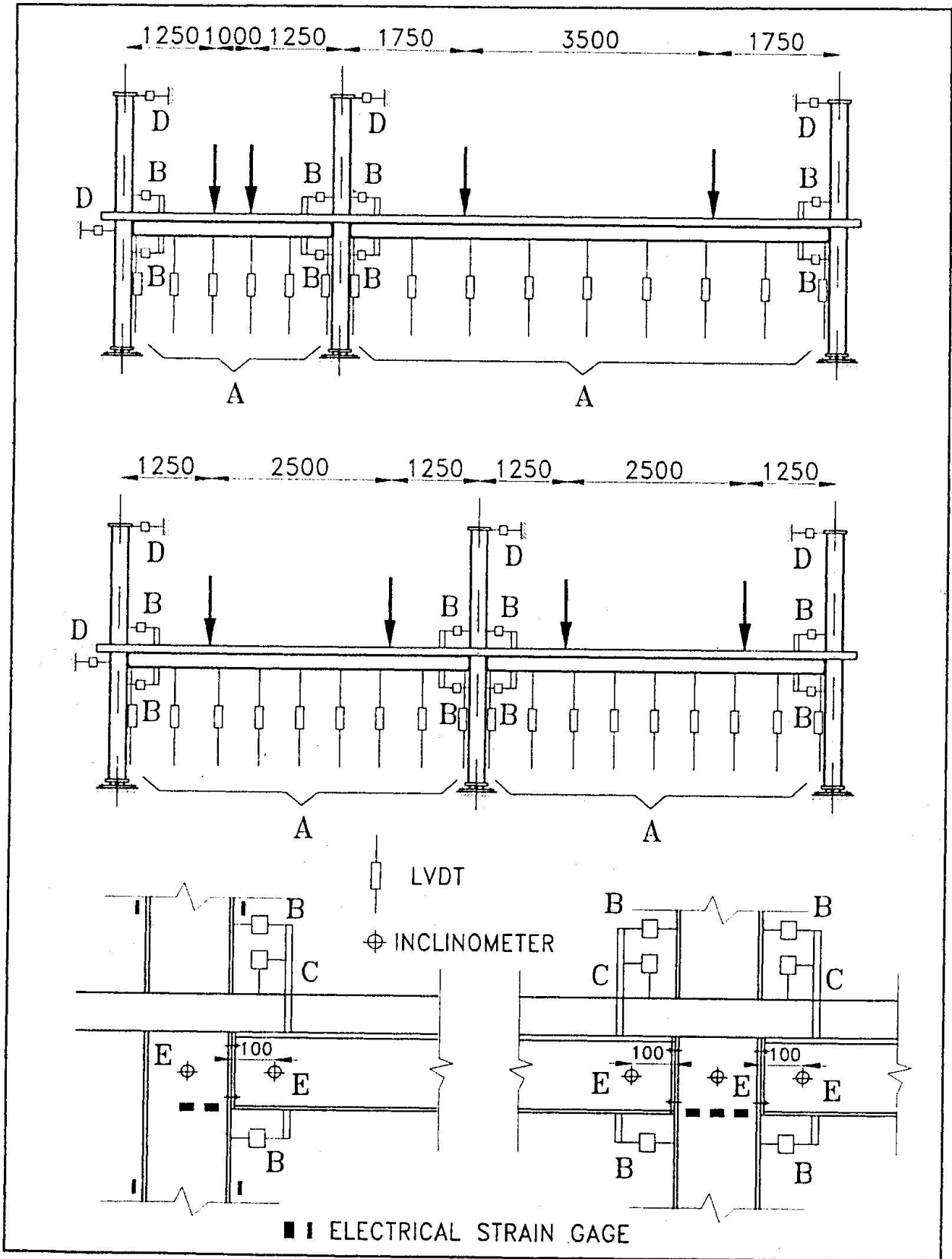


Fig. 4. Instrumentation

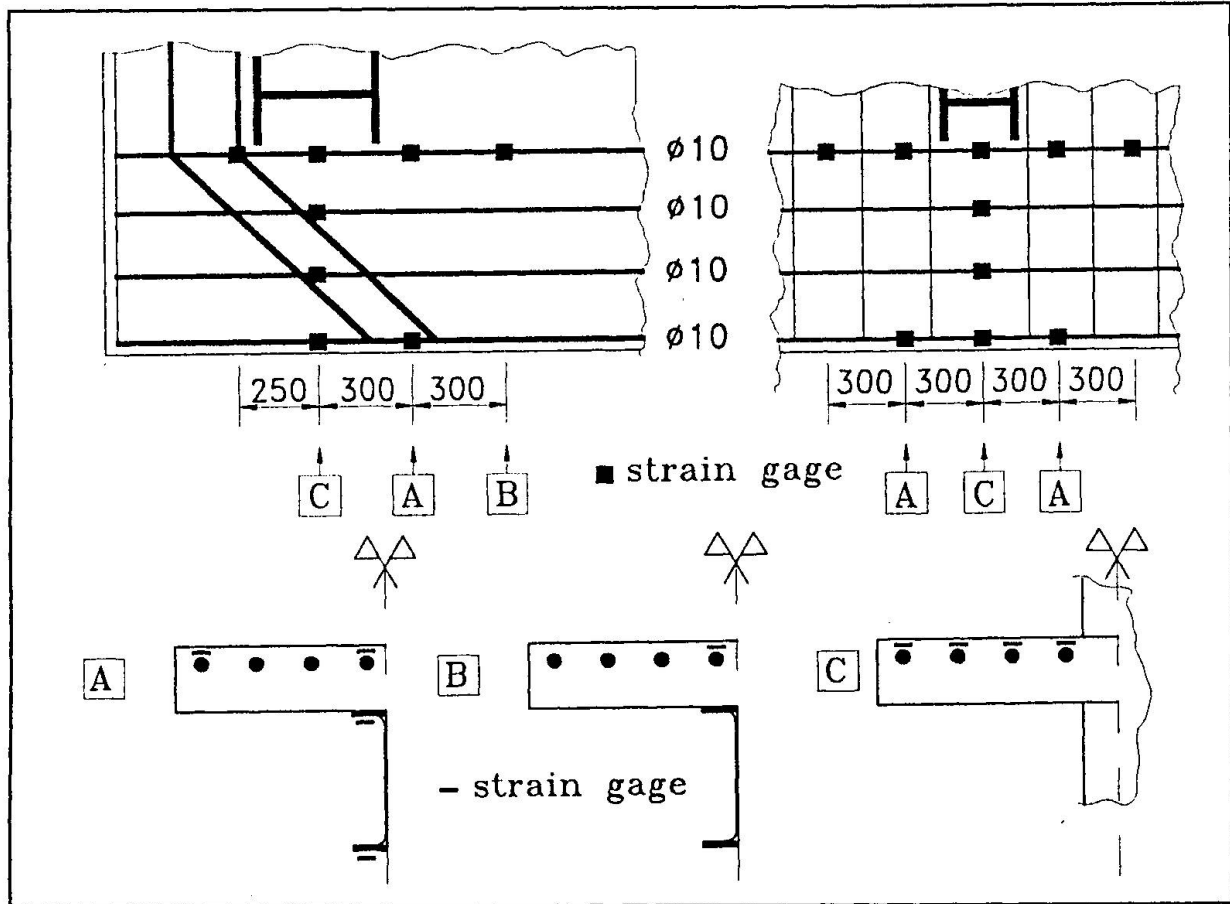


Fig. 5. Strain-gages on slab reinforcement bars.

3. The sub-frames tests

The tests were carried out by assuming the applied loads as control parameter tests and following a step-by-step procedure up to the achievement of the collapse. The loads were applied by subsequent increments at each step and were kept constant until the full development of the deformation was achieved. The loading history comprised several loading cycles with unloading to zero load condition in order to get a more thorough understanding of the structural behaviour.

3.1 Test on sub-frame SCS

The sub-frame specimen SCS was subjected to a symmetrical loading condition. For each composite beams two loads, nominally equal, were applied in accordance with the scheme of fig. 1.

The monitoring of the different joint components showed that internal joints first entered in the plastic range, due to the almost simultaneous yielding both of the inner couple of rebars and of the column panel zone under compression. As a consequence, a rather rapid decrease of joint stiffness was observed and a significant moment redistribution occurred, which lead to the

formation of a plastic hinge at the inner load location of the right beam. Collapse was then attained due to the local buckling at the plastic hinge location. Despite of the important plastic deformations, joints were not involved in the failure mode and did not show any evidence of particular distress. Their rotation capacity proved more than sufficient to ensure the achievement of the beam plastic failure condition. The moment-rotation curves for the internal and for the external joints (fig. 6) showed a remarkable similarity. The internal joints exhibited a noticeable plateau at a lower level of load due mainly to the yielding of the column web panel in compression.

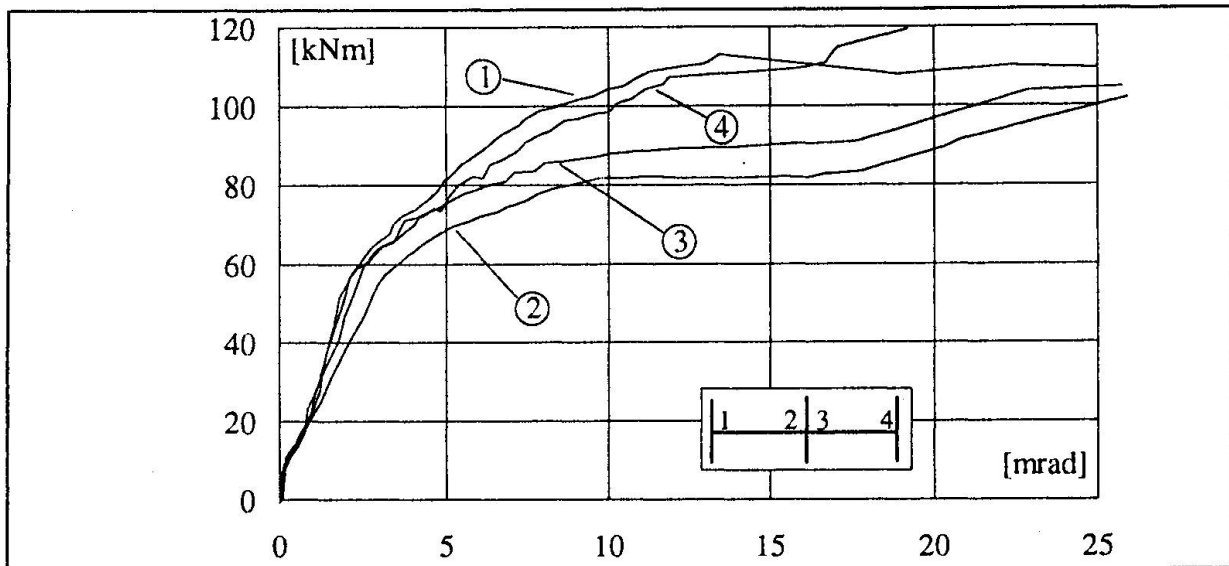


Fig. 6. $M-\phi$ curves for SCS joints

3.2 Test on sub-frame UCS

As previously mentioned, the response of the unsymmetrical composite sub-frame (UCS) was monitored also in the constructing stage [9]. During the concreting of the slab the beams were unpropped and the steel decking was supported for a short period (about 5 days). It appears clearly from fig. 7, in which the strain readings of the internal column (subject to the more severe state of deformations) and the room temperature are reported as a function of the concrete age. The discontinuity at a time of approximately 120 hours corresponds to the removal of the slab propping system. The trend of the strain-time relationships is significantly affected by the shrinkage of the concrete. It is important to note that to the increase in time corresponds a gradual decrease of the slope of the strain readings (in terms of mean values), due to the action of the shrinkage which is more relevant in the first period/immediately after the concreting of the slab. This is also confirmed by the measurements on concrete specimens in the same conditions of the slabs. After 550 hours from concreting the shrinkage deformation value was approximately 2.1×10^{-4} , and it increased up to 2.7×10^{-4} before testing of the sub-frame (about 2 months after the concreting of the slab).

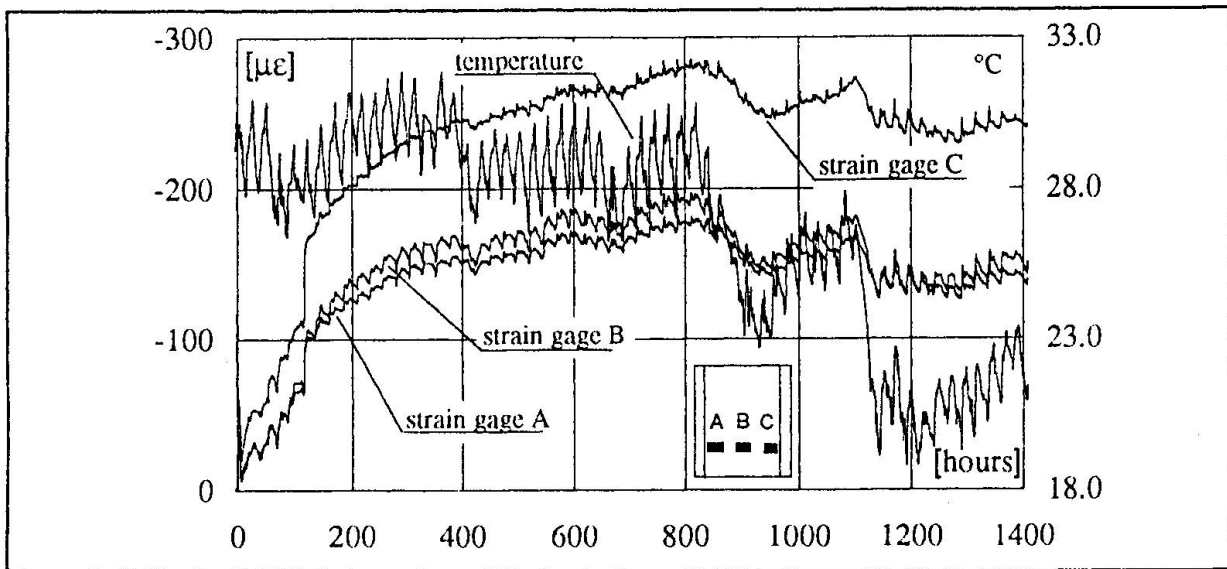


Fig. 7. Strain in the web panel of UCS specimen before the test

An appraisal of the bending moment due to the self-weight of the composite beams and to the shrinkage effects was assessed on the basis of the deformations of the web panel of the columns. As results from fig. 8, the values of the bending moments before the test are non negligible, ranging from 11 to 16 kNm for the internal joints and from 4 to 10 kNm for the external ones, and taking into account that the theoretical values for the cracking and yielding hogging moments of the composite joints are 32 kNm and 92 kNm, respectively.

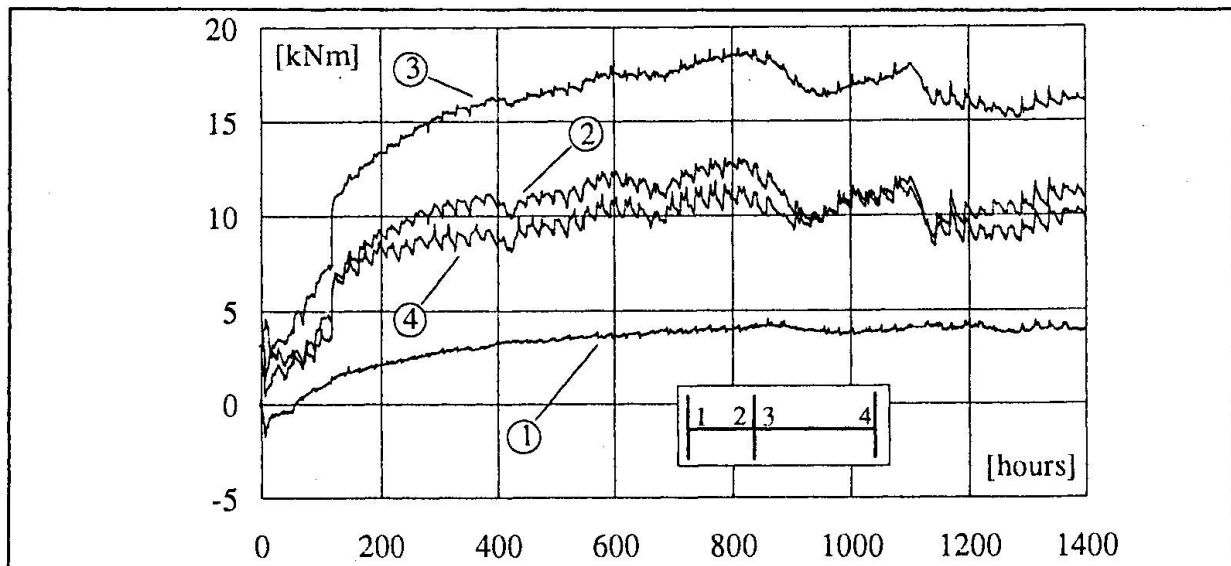


Fig. 8. Bending moments at the joints of UCS specimen before the test

During the test on the unsymmetrical sub-frame, in accordance with the scheme of fig. 1, equal loads were applied on each span until the collapse was achieved on the longer beam. Then the loads on this beam were kept constant by increasing the two loads on the shorter beam. As to the beam with the longer span, the internal joint entered first in the plastic range, exhibiting a noticeable plateau due to the almost simultaneous yielding both of the inner couple of rebars and of the column panel zone under compression. The decrease of joint stiffness and the consequent moment redistribution led to the formation of a plastic hinge at the load location closer to the column. Collapse was caused by local buckling at the plastic hinge location. It should be remarked that before the collapse occurred, relevant slips between the concrete slab and the top flange of the steel beam developed in the zone between the load application points and the internal column.

In the second part of the test, which led to the collapse of the shorter beam the failure mode was similar to that of the longer one. The beam plastic hinge formed at the load location closer to the external column.

The moment-rotation curves for the internal and for the external joints are reported in fig. 9. The curves are obtained by shifting the experimental curves in order to represent, in accordance with fig. 8 for the UCS sub-frame, the joints response due to the sole loads applied during the test (i.e. neglecting the contribution of the concrete shrinkage).

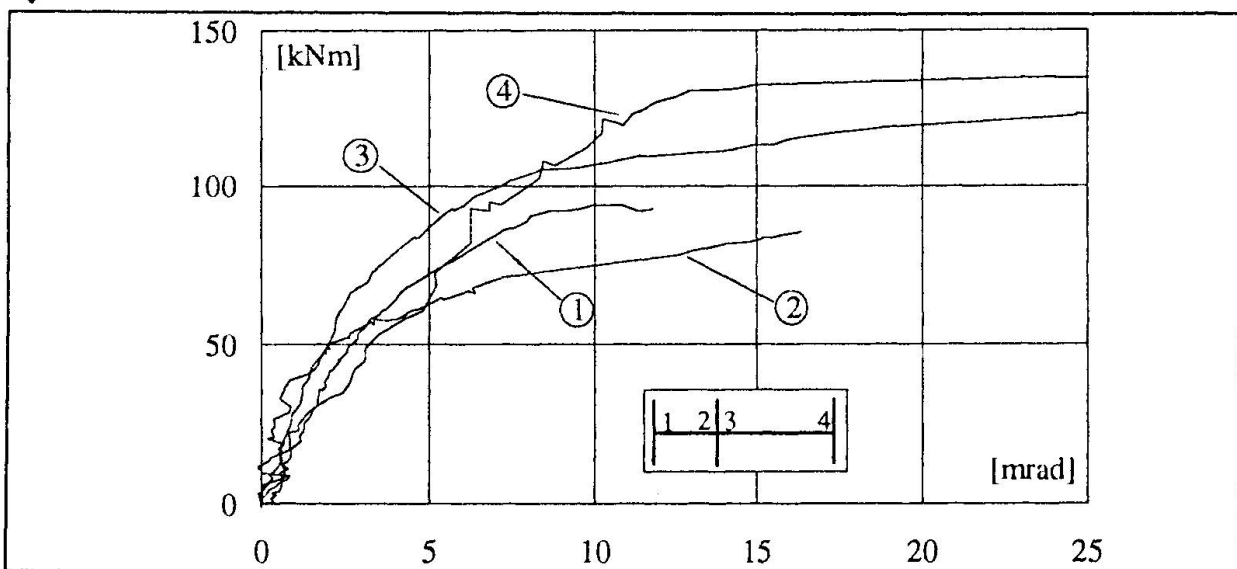


Fig. 9. $M-\phi$ curves for UCS joints

4. Preliminary conclusions

The experimental programme of a joint research project between the Universities of Trento and Trieste is briefly presented together with the main features of the tests carried out on two steel-concrete composite sub-frames. An extensive analysis of the data obtained from the complex measuring system adopted to monitor the behaviour of the tested sub-frames is presently in progress.

The very first results seem to indicate that the joint behaviour is more than satisfactory. Despite the important plastic deformations, joints were not involved in the failure mode, and did not show any evidence of particular distress. Their rotation capacity proved more than



sufficient to ensure the achievement of the beam plastic failure condition. The anchorage detailing of the trimming bars for joints to the external column confirmed a highly satisfactory behaviour.

Finally, with reference to the UCS sub-frame, it is necessary to underline the importance of the shrinkage of the concrete slab to the joints performance.

Acknowledgements

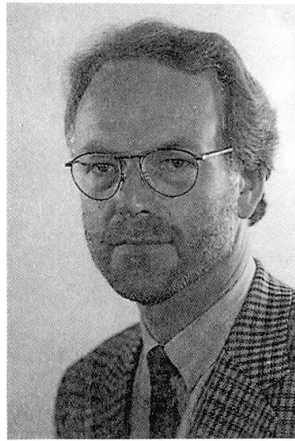
This research was made possible by grants from the Italian Research Council (C.N.R.). The tests were carried out at the Laboratory Prove Materiali of the University of Trieste, through the skilful work of dr. Antonio Rizzo and his technical staff.

References

- [1] Nethercot D.A., Zandonini R., 1994, "Recent Studies of the Behaviour of Semi-Rigid Composite Connections", American Society of Civil Engineers, Structural Conference, Atlanta, April.
- [2] Puhali R., Smotlak I., Zandonini R., 1990, "Semi-Rigid Composite Action: Experimental Analysis and a Suitable Model", Journal of Constructional Steel Research: Special Issue on Composite Construction, R. Zandonini Ed., Vol. 15, Nos 1&2, pp. 121-151.
- [3] Benussi F., Nethercot D.A., Zandonini R., 1995, "Experimental Behaviour of Semi-Rigid Connections in Frames", 3rd International Workshop on Connections in Steel Structures, Trento, May.
- [4] Li T.Q., Moore D.B., Nethercot D.A., 1995, "The Experimental Behaviour of Full-Scale, semi-Rigidly Connected Composite Frames: Detailed Appraisal", in preparation.
- [5] Commission of the European Communities, 1994, "Eurocode 3: Design of Steel Structures: part 1.1 - General Rules and Rules for Buildings".
- [6] Commission of the European Communities, 1994, "Eurocode 4: Design of Steel-Concrete Composite Structures: part 1.1 - General Rules and Rules for Buildings".
- [7] Davison J.B., Lam D., Nethercot D.A., 1988, "Semi-rigid Action of Composite Joints", The Structural Engineer, Vol. 68, No. 24, December, pp. 489-498
- [8] Noè S., 1995, "Tests on Steel-Concrete Composite Subassemblages: Part 1", (in Italian) Laboratory Report, Department of Civil Engineering, University of Trieste.
- [9] Noè S., 1995, "Structural Monitoring of a Semi-Rigid Composite Sub-Frame under Construction", (in Italian) Italian Conference on Steel Structures, Trento, October.

A Consistent Formulation of the Yield-Hinge Theory for 3-D Frames Considering the Deformations of Connections

Dr. Norbert Gebbeken
Engineering Mechanics
& Structural Mechanics
University of the Federal
Armed Forces Munich
85577 Neubiberg
Germany



Professor (chair of EM&SM),
civil engineer,
M.Sc., PhD and Habilitation
from Hannover University,

Summary

As far as steel-rod structures are concerned the yield-hinge theory is a very efficient approach of the ultimate-load theory. The deformability of semi-rigid connections significantly affects the load-carrying behaviour and as a consequence the elasto-plastic failure. In the present paper a formulation of a generalized yield-hinge theory in combination with the consideration of the deformations of connections is consistently developed from the theory of plasticity. The numerical example shows the efficiency of the proposed method.

1 Introduction

The harmonization of the national and international standards will affect the design of steel structures in the future. Due to the reasons of safety and economy it is advised to apply methods which allow to consider the nonlinear geometrical effects as well as the nonlinear material behaviour. As far as frames are concerned the *yield-hinge theory* is widely accepted. Earlier proposed methods, e.g. GREENBERG & PRAGER ([5]), were restricted to the geometrical nonlinear theory of second order (*theory of 2nd order*) or by considering just $P - \delta$ -effects ($P - \delta$ -method). Moreover, the plastic behaviour was only considered in regard to the bending moment. A few authors took the *interaction* of the internal forces in the plastic regime into account. Thus, yielding an inconsistent theory as shown in [3]. In order to derive an advanced numerical procedure for the yield-hinge theory the above-mentioned simplifications are not necessary.

Yield-hinge theory methods can be subdivided into two main branches: *concentric-yield hinge theory* and *eccentric-yield hinge theory (generalized yield-hinge theory)*. The main advantage of any yield-hinge approximation is based on its economical application from



the computational point of view and on its vivid derivation (GEBBEKEN [3]). Studies have shown that the *yield-hinge theory* represents the *load-carrying behaviour* of frames sufficiently for a wide range of applications.

In this paper both, the theory and its numerical treatment in context of the finite element method are presented in order to determine the nonlinear elasto-plastic load-carrying behaviour and the ultimate load of frames. In addition, this contribution focusses on developing a practice related method.

2 Fundamentals of the yield-hinge theory

The assumptions of the yield-hinge theory of beams are almost identical to the assumptions of the classical rod-theory (LUMPE [6]). The frames comprise of more or less slender, prismatic and straight steel members with *rigid or semi-rigid structural connections* at the joints. In the three-dimensional case the numerical node has six degrees of freedom which are the *nodal displacements* and the *nodal rotations* associated to the six *nodal forces*. *Yield-hinge models* are introduced for the purpose of representing the actual plastic deformations as well as the actual ultimate load-carrying capacity of beam members.

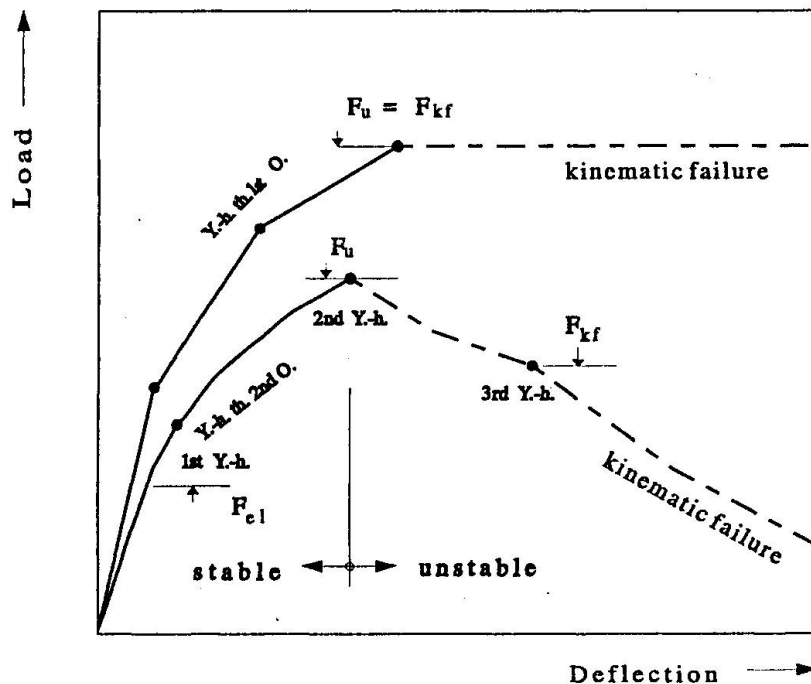


Figure 1: Comparison of load-deflection curves

The *limit points* (Fig. 1) of the yield-hinge theory can be defined with the help of the following four **limit-load conditions**:

1. equilibrium exists,
2. the yield-condition of a cross-section is not violated,
3. the virtual work on the path of plastic deformations is not negative,
4. the kinematic mechanism (failure mode) of the system is attained.

The first three conditions define the *ultimate-load* (F_u) while all four conditions define the *kinematic-failure load* (F_{kf}). The *ultimate-load* (F_u) is the maximum-load which a structure can be subjected to. The ultimate-load might be detected as buckling-load due to elasto-plastic loss of stability. The *kinematic-failure load* (F_{kf}) is associated to the plastic failure of the structure going along with the forming of a mechanism. Applying the yield-hinge theory of first order (geometrical linear theory) the values of F_{kf} and F_u are identical. Applying a geometrical nonlinear theory $F_{kf} \leq F_u$ holds. The consideration of the geometrical nonlinearity is a requirement to carry out stability analyses. It is a necessary condition that the virtual work of the plasticized cross-sections is not negative. This is guaranteed if *incremental procedures* and the generalized yield-hinge concept are applied. The *interaction of the internal forces* in plasticized cross-sections is described by *interaction-functions* f (*yield-functions*) which are based on the J_2 -flow theory.

3 Mathematical formulation of the yield-surface

We postulate a function

$$f = f(F_i, k) \begin{cases} > 0 & \text{hardening} \\ = 0 & \text{yield-condition (elastic limit)} \\ < 0 & \text{elastic regime} \end{cases} \quad (1)$$

where F_i are the (ultimate) internal forces and k is a parameter that comes from the yield-criterion. The function f defines the *limit-state of elasticity* under any possible combinations of *ultimate stress-resultant components (ultimate internal forces)*. For this, the *yield-criterion* of HUBER, v. MISES & HENCKY (J_2 -flow theory) is best suited to simulate the elastic limit of steel. The equation $f = 0$ defines the transition (elastic limit or beginning of plastification) between the elastic ($f < 0$) and the plastic ($f \geq 0$) regime. The inequation $f > 0$ represents hardening of the material which is not considered here. In the framework of the limit-load theory of frames, the yield-function is often called "interaction-function".

The problem of formulating interaction-functions has been tackled by many scientists in the last three decades. A large number of different interaction-functions have been proposed in the literature. A survey and a comparison have been published in [1].

RUBIN derived in [8] *interaction-functions* which represent the *yield-surface (yield-locus)* of open rectangular cross-sections and double-T cross-sections. The derivations are carried out under consideration of all internal forces, except of the torsional moment. Thus, yielding an exact representation of the yield-surface in the case of plane bending, and a fairly



good approximation of the three-dimensional case. The influence of the torsional component can be approximately considered by adding the value of the stress due to torsion to the shear-stress. As far as it is known from the literature, only the interaction-functions of RUBIN are strictly derived from admissible ultimate stress states of full plasticized cross-sections. So, they can be seen as the most accurate ones.

For practical purposes simplified empirical interaction-functions on different approximation levels have been proposed. *Empirical interaction-relations* are not necessarily derived from the integration of stress-states. Their mathematical structure is often very simple. These formulae serve to approach the true *ultimate-load capacity* of a cross-section which is represented by the *yield-surface*.

In order to fulfill the condition of convexity of the yield-surface (DRUCKER's *postulation*) a *lower bound of the yield-surface* is defined by

$$f = \left| \frac{M_y}{M_y^p} \right| + \left| \frac{M_z}{M_z^p} \right| + \left| \frac{N}{N^p} \right| - 1 = 0 \quad . \quad (2)$$

Eq. 2 represents a plane in the three-dimensional space of M_y , M_z , N . The influence of the shear-forces is here considered according to RUBIN. Eq. 2 is the most simple yield-function. The influence of the torsional component can be approximately considered by adding an extra term $(M_x/M_x^p)^2$ to the left-hand side of the yield-function. For more information about interaction formulae see [1].

4 On the yield-hinge concepts

4.1 Concentric yield-hinges

The most simple possibility to represent plastic load-carrying behaviour is the introduction of *concentric yield-hinges*. In textbooks we can find applications to pure bending or pure membrane or pure shear, respectively. Thus, concentric yield-hinges associated with bending moment or normal-force or shear-force are introduced. The symbols for these concentric yield-hinges are given in Fig. 2.

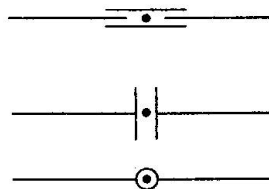


Figure 2: Symbols for concentric yield-hinges: 1st) normal-force, 2nd) shear-force, 3rd) bending moment

For frame analysis it is widely accepted to apply concentric yield-hinges associated with the bending moment. This is the *classical strategy*. For the analysis of *truss-structures* it

is obvious to apply concentric yield-hinges with respect to the normal-force (*normal-force yield-hinge*). For details see [1], [7].

The implementation of concentric yield-hinges into a computer program can easily be achieved by the technique of *static condensation* with respect to the nodal displacement component. Thus, yielding a plastic stiffness matrix for the beam and an additional nodal vector on the right-hand side which includes the plastic nodal forces. Within this procedure, the *yield-condition* can be considered with the help of an inner iterative loop. *It is worth-mentioning that, in any case, these concentric yield-hinges are located in the centerline of the beam and not in the neutral axis.*

4.2 Eccentric yield-hinges

GIRKMANN already pointed out in 1932 ([4]) that the position of a yield-hinge moves in thickness direction of a cross-section and that the position coincides with the location of the neutral axis. In the following we will derive a closed and theoretical consistent formulation for *two-dimensional and three-dimensional frames*. The kinematic relations are drawn in Fig. 3 for the two-dimensional case and in Fig. 4 for the three-dimensional case.

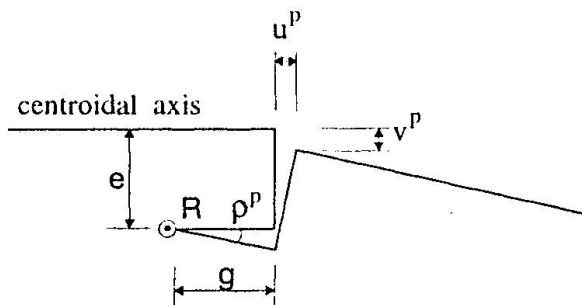


Figure 3: Generalized (eccentric) yield-hinge (two-dimensional)

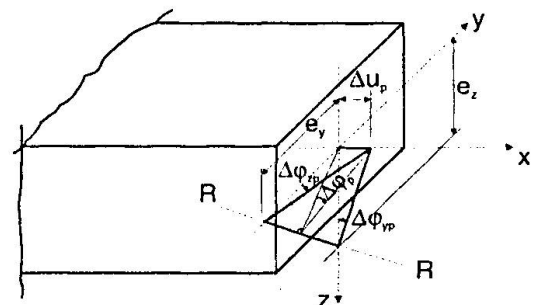


Figure 4: Generalized (eccentric) yield-hinge (three-dimensional)

The formulation for yield-hinges is carried out in the framework of a geometrical nonlinear formulation. Because of the incremental, iterative procedure the relations are linearized for each iterative step. Consequently, we can start with the linear relation between the *nodal force vector* and the *nodal displacement vector* in the elastic regime.

$$F = k v^e \tag{3}$$

In order to consider the plastification at the end nodes *i* and *j* of a rod it makes sense to write Eq. 3 explicitly with respect to both end nodes:

$$F = \begin{bmatrix} F_i \\ F_j \end{bmatrix}^{12} = \begin{bmatrix} k_{ii} & k_{ij} \\ k_{ji} & k_{jj} \end{bmatrix}^{12} \begin{bmatrix} v_i^e \\ v_j^e \end{bmatrix}^{12} \tag{4}$$



For elasto-plastic analysis we have to add the plastic deformation as well as the deformation of the connections, or vice versa, the total incremental displacement vector Δv can be decomposed additively into an elastic part Δv^e , a plastic part Δv^p , and a part Δv^d due to the deformability of semi-rigid connections,

$$\Delta v = \Delta v^e + \Delta v^p + \Delta v^d \quad , \quad (5)$$

$$\Delta v = \begin{bmatrix} \Delta v_i \\ \Delta v_j \end{bmatrix}^{12} = \begin{bmatrix} \Delta v_i^e \\ \Delta v_j^e \end{bmatrix}^{12} + \begin{bmatrix} \Delta v_i^p \\ \Delta v_j^p \end{bmatrix}^{12} + \begin{bmatrix} \Delta v_i^d \\ \Delta v_j^d \end{bmatrix}^{12} \quad , \quad (6)$$

respectively. Applying an incremental procedure the following holds for each increment:

$$f + \Delta f = f(F_i, k) + \Delta f(\Delta F_i, k) = 0. \quad (7)$$

Provided that the yield-condition $f = 0$ (1) holds, it is a result of (7) that the incremental part of the yield-condition has to be fulfilled by the increment of the nodal force vector. Assuming an ideal plastic material behaviour it is evident that the incremental part of the nodal force vector is part of the yield-surface $f = 0$. Rearranging and inserting (6) into (4) we obtain

$$\Delta F = \begin{bmatrix} \Delta F_i \\ \Delta F_j \end{bmatrix}^{12} = \begin{bmatrix} k_{ii} & k_{ij} \\ k_{ji} & k_{jj} \end{bmatrix}^{12} \begin{bmatrix} \Delta v_i^e \\ \Delta v_j^e \end{bmatrix}^{12} = \begin{bmatrix} k_{ii} & k_{ij} \\ k_{ji} & k_{jj} \end{bmatrix}^{12} \begin{bmatrix} \Delta v_i - \Delta v_i^p - \Delta v_i^d \\ \Delta v_j - \Delta v_j^p - \Delta v_j^d \end{bmatrix}^{12} \quad .(8)$$

Since we have introduced the plastic deformation vector and the deformation vector of the connections explicitly, we need a rule how to determine them. For the **plastic deformation**, we apply the well established *flow-rule* of PRANDTL and REUSS:

$$\Delta v^p = \lambda^p \frac{\partial f}{\partial F_i} = \lambda^p \nabla f \quad , \quad \lambda^p \geq 0 \quad (9)$$

or written with respect to each node

$$\Delta v_i^p = \lambda_i^p \nabla f_i \quad , \quad (10)$$

$$\Delta v_j^p = \lambda_j^p \nabla f_j \quad , \quad (11)$$

respectively, where λ_i^p and λ_j^p are proportional constants (*plastic multiplier*). For this, it is assumed that the yield-function f is a potential.

Annotation: *This is the decisive extension to the concentric yield-hinge concept. With the flow-rule (9) the material formulation is complete and consistent to the theory of plasticity.*

For the **deformation of the connections**, we apply the moment-rotation relations expressed by

$$\Delta v^d = \lambda^d M \quad (12)$$

or written with respect to each node

$$\Delta v_i^d = \lambda_i^d M \quad , \quad (13)$$

$$\Delta v_j^d = \lambda_j^d M \quad , \quad (14)$$

respectively, where λ_i^d and λ_j^d are the secant stiffnesses of the moment-rotation graphs. They can be produced by experimental investigations or by numerical analyses as shown in GEBBEKEN et al. [2].

Finally we arrive at

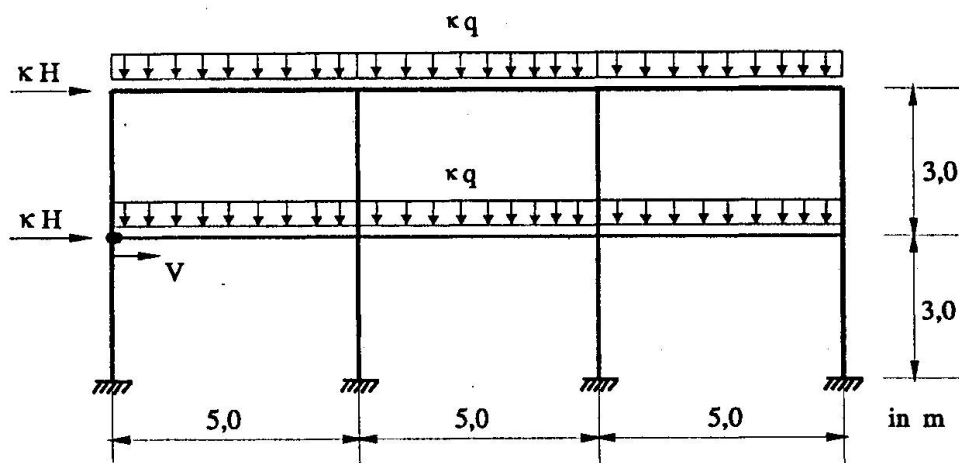
$$F = \begin{bmatrix} F_i \\ F_j \end{bmatrix}^{12} = \begin{bmatrix} k_{ii}^{pd} & k_{ij}^{pd} \\ k_{ji}^{pd} & k_{jj}^{pd} \end{bmatrix}^{12} \begin{bmatrix} v_i \\ v_j \end{bmatrix}^{12} \quad , \quad (15)$$

where $[k^{pd}]$ is the *element stiffness matrix* for an elasto-plastic rod element with semi-rigid connections.

5 Numerical Example

Two storey four bay plane frame

The frame chosen for analysis is shown in Fig. 5. This structure has been firstly investigated by STUTZKI in [9]. It is assumed that all girders are semi-rigidly connected to the columns.



$q = 60.0 \text{ kN/m}$ Beams: HEB 300
 $H = 31.0 \text{ kN}$ Columns: HEA 220
 Material: Fe 360 B (St 37-2)

Figure 5: 2-D Frame: Geometrical data, yield-stress and loading



In order to illustrate the influence of the deformation of connections on the nonlinear effects, STUTZKI used different types of models for the joints. All of them are truss-like models which are vivid but costly with respect to elementation. The stiffness of a truss member serves to simulate the moment-rotation behaviour of the connection under consideration. For the author's calculation, generalized yield-hinges have been used. The numerical models of the connections are now element-inherent, quasi a makro model. Thus, the structural analyst can element the structure as usual. He only needs to define the moment-rotation behaviour of the semi-rigid connection as shown in Fig. 6. In addition, the yield-function (2) and the interaction formulae according to RUBIN are utilized. In order to compare the results, the computations have been carried out for rigid connections as well as for semi-rigid connections with the characteristics shown in Fig. 6.

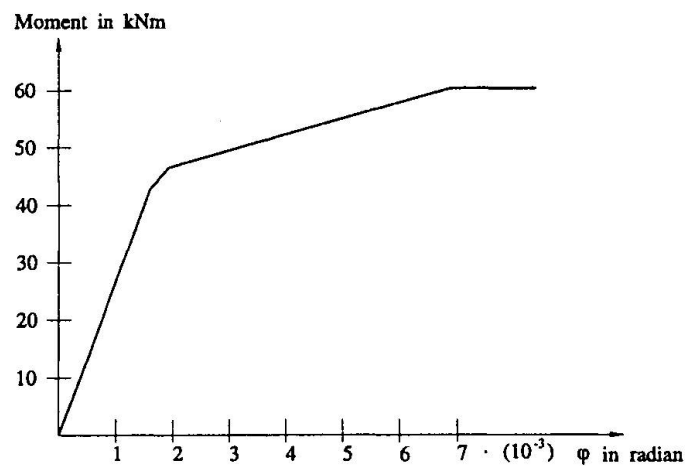


Figure 6: 2-D Frame: Moment vs. rotation graph

The load vs. deflection curves are plotted in Fig. 7 with respect to the horizontal deflection v as shown in Fig. 7. It is obvious that the stiffer the connections the stiffer the load vs. deflection characteristic. Thus, the three upper graphs represent the behaviour of the frame with rigid connections. The solid line has been taken over from STUTZKI whereas the broken lines are the results of the author's calculation. Their deviations are due to the application of different interaction functions. Applying the linear interaction formula the ultimate load is underestimated, while using RUBIN's formulae the ultimate carrying capacity of cross-sections is quite well approximated.

The studies result in a load factor of $\kappa \approx 2.0$ and in a horizontal deflection of the first girder of $\kappa \approx 3.0$ cm. Slender columns, large column compressive axial loads and the influence of the geometrical nonlinearity resulted in a significant reduction of the magnitude of the ultimate load factor (from $\kappa \approx 2.0$ to $\kappa \approx 1.6$) when compared to the analysis with rigid connections. Only 80% of the first-order ultimate load was attained. Besides the nonlinear moment-rotation behaviour of the connections the members partly suffer plastifications.

The results show clearly that the frame studied here is a member of the so-called "second order frame" family. Due to the influence of the deformations on the equilibrium formu-

lation, these frames usually failed by elasto-plastic instability prior to the formation of a plastic mechanism.

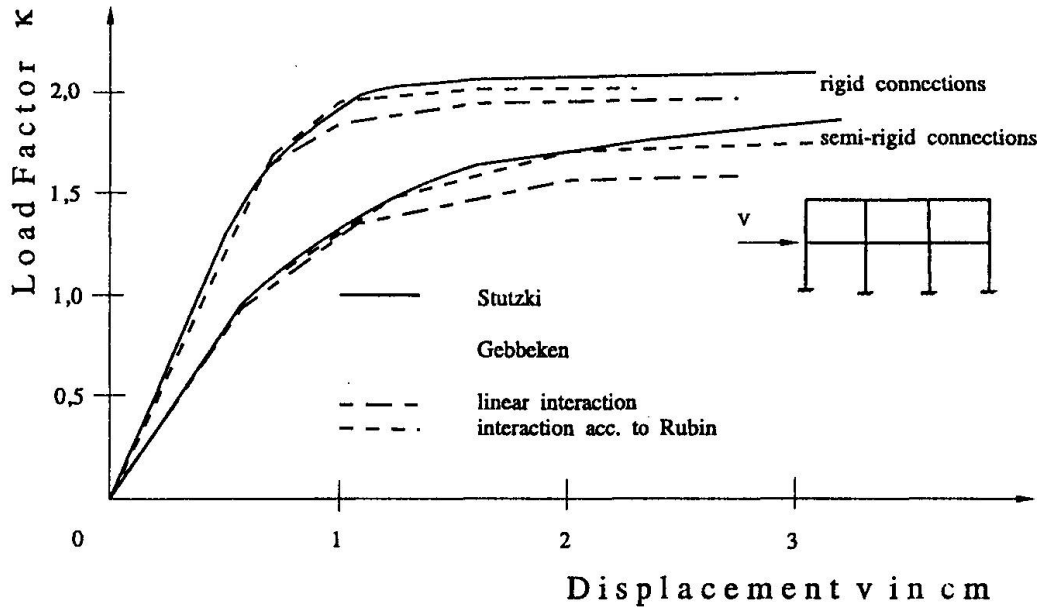


Figure 7: 2-D Frame: Load vs. deflection curves

According to the German standard DIN 18800 we have to consider safety factors in order to design the frame. The safety factor for the loads is $\gamma_F = 1.5$ and the safety factor for the material is $\gamma_M = 1.1$. Thus, we can predict a design load factor of $\kappa_D = 1.06$. The frame with semi-rigid connections has a total weight of $W = 47.22 \text{ kN}$. The elastic limit-load has been reached at $\kappa_D = 0.9$. Consequently, we need HEB 220 profiles for the columns which results in a total weight of $W = 52.26 \text{ kN}$. Assuming that the members are rigidly connected to each other HEB 280 profiles are sufficient for the girders. In this case a total weight of $W = 43.02 \text{ kN}$ has been calculated. This comparison reveals that on the one hand it is economical to apply nonlinear methods, on the other hand it is a demand to apply nonlinear methods in order to guarantee safety.

Annotations:

The magnitude of the ultimate-load depends significantly on the deformability of the connections as well as on the used interaction-function. If the structure turns to be weak due to geometrical nonlinear effects as well as due to plastification, the calculation is very sensitive with respect to the deformations. The method is robust regarding the ultimate loads.



References

- [1] Gebbeken, N.: *Eine Fließgelenktheorie höherer Ordnung für räumliche Stabwerke - Zugleich ein Beitrag zur historischen Entwicklung*, Mitt. Nr. 32-88, Inst. für Statik, Universität Hannover, 1988 and Stahlbau 57 (1988) 365-372
- [2] Gebbeken, N.; Rothert, H.; Binder, B.: *On the Numerical Analysis of Endplate Connections*. Journal of Constructional Steel Research, 30 (1994) 177-196
- [3] Gebbeken, N.: *A Refined Numerical Approach for the Ultimate-Load Analysis of 3-D Steel Rod Structures*, submitted to Engineering Computations, (1996)
- [4] Girkmann, K.: *Über die Auswirkung der "Selbsthilfe" des Baustahls in rahmenartigen Stabwerken*. Der Stahlbau 5 (1932) 121-127
- [5] Greenberg, H.J.; Prager, W.: *On the limit design of beams and frames*. Proc. ASCE 77 No. 59 (1951)
- [6] Lumpe, G.: *Geometrisch nichtlineare Berechnung von räumlichen Stabwerken*, Mitt. Nr. 28, Institut für Statik, Universität Hannover, 1982
- [7] Rothert, H.; Gebbeken, N.: *On Numerical Results of Reticulated Shell Buckling*. Int. J. of Space Structures 7, No. 4 (1992) 299-319
- [8] Rubin, H.: *Interaktionsbeziehungen für doppelsymmetrische I- und Kastenquerschnitte bei zwiachsiger Biegung und Normalkraft*. Der Stahlbau (1978) 145-151, 174-181
- [9] Stutzki, C.: *Traglastberechnung räumlicher Stabwerke unter Berücksichtigung verformbarer Anschlüsse*. Institut für Stahlbau, RWTH Aachen (1982)